Mathematical Frameworks of All-Quantum Mode Adaptable Communication Processors

DONYA SADAT REZAEISHAD,[1,2] MOHAMMAD REZAI,[2,3] FOROOGH SADAT TABATABA,[1] AND JAWAD A. SALEHI[2,3,4]

[1] *Department of Electrical and Computer Engineering, Isfahan University of Technology, Isfahan 84156-83111, Iran*
[2] *Sharif Quantum Center, Sharif University of Technology, Tehran 14588-89694, Iran*
[3] *Center for Quantum Science and Technology, Institute for Convergence Science and Technology, Sharif University of Technology, Tehran 14588-89694, Iran*
[4] *Department of Electrical Engineering, Sharif University of Technology, Tehran 11155-4363, Iran*

Abstract: The diversity of quantum communication protocols and their rapid growth entail the development of the Quantum Internet, the interconnection of various quantum communication nodes and systems. One of the challenges posed by this development is all-quantum mode adaptation, which is essential for adapting different quantum nodes to the common network, enhancing the efficiency and scalability of quantum information transmission. This paper investigates the mathematical frameworks of all-quantum mode adaptation, focusing on three essential elements—mode expansion, mode reduction, and mode mapping—which are crucial for managing compatibility among different quantum signals. By leveraging various degrees of freedom of photons, we demonstrate the possibility of adaptable all-quantum processors that can dynamically adjust to different communication environments, addressing real-world challenges in the Quantum Internet.

1. Introduction

The rapid advancement of quantum communication technologies has opened new opportunities in quantum computation and processing science. This progress enables the execution of complex algorithms and operations that are unattainable by classical processors. Quantum processors leverage the unique properties of quantum mechanics, such as superposition and entanglement, to perform computations and facilitate communication at unprecedented security levels [1, 2]. However, effective operation relies on the seamless adaptability of quantum signals—essential for ensuring compatibility both within the quantum processor and across different devices in a quantum network, as illustrated in Fig. 1.

To be more specific, quantum information and its processing are implemented in various physical systems, depending on the application and specific conditions. Essentially, quantum information is represented through various quantum signal realizations such as atomic systems [3], superconductors [4], and optical quantum signals [5]. Consequently, in an all-quantum network, the interconnection between these quantum signals and their conversion into one another—referred to as quantum signal adaptability—is vital.

Focusing specifically on optical quantum signals, quantum light offers multiple platforms for quantum computation and communication, such as path or propagation line [6], polarization [7–9], frequency [10, 11], and time domains [12–14]. Therefore, in an all-quantum optical network, the interaction among these different optical implementations of quantum information becomes important. For instance, the interplay between quantum computers processing information in the path domain [15, 16] and those operating in the time and frequency domains [17, 18], as well as the protocols encoded in the polarization domain [19, 20], underscores the significance of what

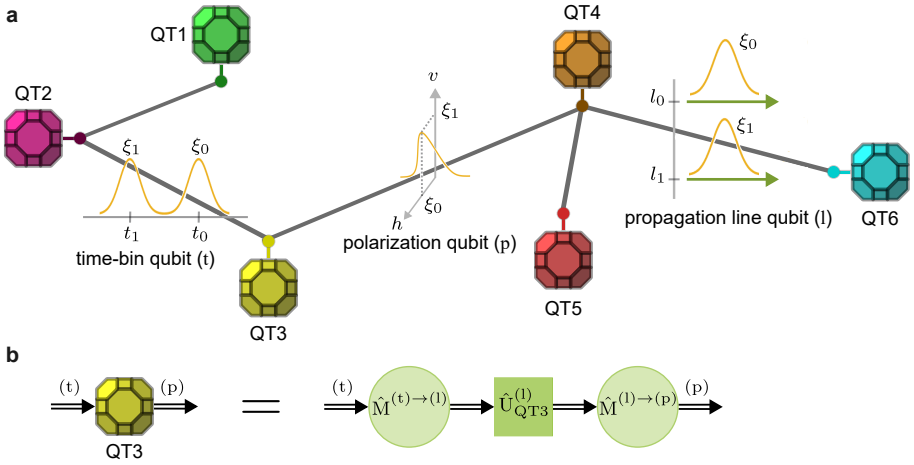

Fig. 1. All-quantum mode adaptable communication processors enabling interoperability across various devices in a quantum network and within individual devices. **a** A quantum network with six quantum transceivers (QTs) and different photonic signal modes. Each transceiver must deal with various signal modes within a quantum network with diverse devices. **b** A quantum transceiver may use necessary mode mappings to adapt to signal modes from different input/output channels. In part b, the square indicates a unitary operation, whereas circles signify all-quantum mode mapping operators.

we call mode adaptability. Figure 1-a illustrates the mode adaptability of different processors within a diverse quantum network that handles various optical quantum signals. In Fig. 1-b, we exemplify the third quantum transceiver (QT3), which receives time-bin qubits (t) at the input channel, processes them in the path (propagation line l) domain, and subsequently maps the output quantum information to the polarization qubits (p) that are suitable for transmission through the output channel. Consequently, appropriate mode mapping modules are utilized to transform the input mode (t) into the processing mode (l) and to convert the processing mode (l) into the output mode (p), which will be discussed in detail throughout this paper.

The necessity for mode adaptable all-quantum processors is becoming increasingly apparent as the demand for the interplay between different quantum devices grows. All-quantum mode adaptable processors may find applications in various domains, including quantum algorithms [21–23], quantum key distribution (QKD) [1,24–29], superdense coding [30], quantum teleportation [31], quantum secret sharing [32,33], and quantum secure direct communication (QSDC) [34–36]. Each of these quantum applications requires processors that incorporate quantum operators capable of acting on specific signal states, which must be adapted to other processors' signal modes to enable interoperability among different processors.

This paper explores the potential of all-quantum mode-adaptable processors that leverage various degrees of freedom of photons—including polarization, time, and path characteristics—to enhance the efficiency and scalability of quantum information transmission. By providing a comprehensive analysis of mode expansion, reduction, and mapping techniques, this paper establishes a foundation for future advancements in quantum communication and cooperation. The exploration of all-quantum mode adaptation techniques—which involve controlling and adjusting the various photons' degrees of freedom—is not merely theoretical but essential for practical and scalable quantum communication solutions. The interaction among different quantum signals can aid in encoding and decoding, while also enhancing the success probability of quantum computational gates by facilitating the use of appropriate modes within the structure.

Ultimately, the insights gained from this research may lead to more resilient and versatile quantum communication frameworks, improving the prospects for robust quantum data exchange in an increasingly interconnected all-quantum network [37].

2. Mathematical Foundations for All-Quantum Signal Manipulation

Among various physical systems for quantum information encoding, photons are the most commonly used medium for quantum communications, owing to their resilience to decoherence from noisy environments and their high speed of propagation. Photonic quantum information processing can be implemented using various degrees of freedom of photons, such as quadrature components [38–40], polarization [7–9], time [12–14, 41, 42], frequency [10], spatial modes including orbital angular momentum (OAM) [43, 44], and path (fiber core) bins [45]. However, it is important to recognize that these degrees of freedom are not necessarily independent of one another. Each of these degrees of freedom can be used to carry quantum information, and is referred to as the signal's mode, or simply the mode.

Mathematically speaking, a qudit, which is a d-dimensional unit of quantum information, can be expressed by the quantum state

$$\left|\psi\right\rangle = \sum_{i=0}^{d-1} \xi_i \left|i\right\rangle_L , \tag{1}$$

where $|i\rangle_L$ indicates the i-th logical orthonormal basis state and ξ_i denotes its corresponding probability amplitude, satisfying the following normalization relation

$$\sum_{i=0}^{d-1} |\xi_i|^2 = 1. \tag{2}$$

The qudit described in Eq.(1) can have various optical quantum signal realization. Assume, the information is encoded in mode m, for example, polarization (m = p), time-bin (m = t), and propagation line (m = l). Therefore, the physical state of the quantum information, Eq.(1), has the following quantum signal representation

$$\left|\psi^{(\mathrm{m})}\right\rangle = f\left(\hat{a}_{\xi}^{\dagger(\mathrm{m})}\right)|0\rangle = f\left(\sum_{i=0}^{d-1} \xi_i \hat{a}_{m_i}^{\dagger}\right)|0\rangle , \tag{3}$$

where $f\left(\hat{a}_{\xi}^{\dagger(\mathrm{m})}\right)$ is an analytic and infinitely differentiable function that describes the Fock state representation of the quantum light as a function of the creation operator $\hat{a}_{\xi}^{\dagger(\mathrm{m})}$ [46, 47], and the superscript (m) highlights that the mode m is the carrier of quantum information. For instance, for a coherent (Glauber) state with complex amplitude α, the function that delineates this state is articulated as follows [46, 48, 49]

$$f_{\alpha}\left(\hat{a}_{\xi}^{\dagger(\mathrm{m})}\right) = e^{-\frac{|\alpha|^2}{2}} e^{\alpha\, \hat{a}_{\xi}^{\dagger(\mathrm{m})}}, \tag{4}$$

where the average number of photons in the state is $|\alpha|^2$. In contrast, for a single photon, the function is defined as the identity function, as demonstrated in the following expression

$$f(\hat{a}_{\xi}^{\dagger(\mathrm{m})}) = \hat{a}_{\xi}^{\dagger(\mathrm{m})}. \tag{5}$$

In the multi-mode encoding, the information is encoded in the occupation mode of photons. For instance, in Eq.(3), the i-th probability amplitude of the qudit (Eq.(1)) is encoded in m_i, the

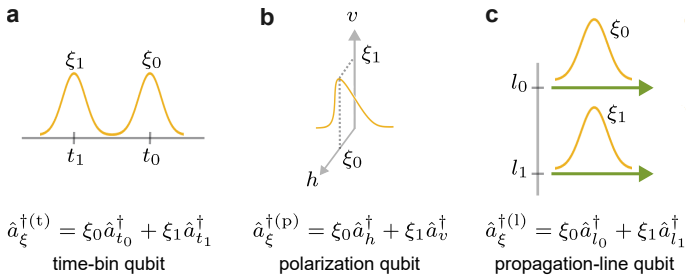

Fig. 2. Representation of qubit encoding through various degrees of freedom of a photon with $|\xi_0|^2 + |\xi_1|^2 = 1$. **a** Time-bin qubit; **b** Polarization qubit; **c** Propagation-line qubit.

i-th vector basis of the photonic mode m. Since there is no information encoded in the other independent modes, we omit them and have chosen to explicitly specify only the mode m. This simplifies the expression of the quantum signal and highlights the relevant mode m that carries the quantum information.

For example, consider temporal logical qubit encoding, i.e., m $\rightarrow$ t, and $d = 2$. Thus, Eq.(3) converts to

$$\left|\psi^{(\mathrm{t})}\right\rangle = f\left(\hat{a}_\xi^{\dagger(\mathrm{t})}\right)|0\rangle = f\left(\xi_0 \hat{a}_{t_0}^\dagger + \xi_1 \hat{a}_{t_1}^\dagger\right)|0\rangle\,, \tag{6}$$

where

$$|\xi_0|^2 + |\xi_1|^2 = 1. \tag{7}$$

Note that in Eq.(6), the modes that are not explicitly written, such as polarization and spatial modes, are assumed to remain preserved and identical for time-bins t_0 and t_1. However, for each single photon, the temporal modes t_0 and t_1 have different probability amplitudes associated with the quantum bit of information of Eq.(1). Figure 2 illustrates the distinct approaches to qubit encoding through various degrees of freedom of a photon, specifically highlighting time-bin, polarization, and propagation-line qubits.

2.1. *Intra-Mode Unitary Operation*

Applying a unitary operator $\hat{\mathrm{U}}$ with matrix elements $u_{i,j}$ located in the i-th row and j-th column results in the following expression

$$\left|\psi'\right\rangle = \hat{\mathrm{U}}\left|\psi\right\rangle = \sum_{i=0}^{d-1} \xi_i' \left|i\right\rangle_L\,, \tag{8}$$

where

$$\xi_i' = \sum_{j=0}^{d-1} u_{i,j}\ \xi_j. \tag{9}$$

In multi-mode encoding, the Fock state representation of quantum light, denoted by function f, carries no quantum information. Furthermore, it remains unchanged when subjected to linear optical devices that affect only the photonic mode m, for example, half-wave plate for polarization encoding (m = p) or beam-splitter for propagation line encoding (m = l). Such linear optical devices can be expressed with intra-mode unitary operator $\hat{\mathrm{U}}^{(\mathrm{m})}$. Consider applying a unitary

operator $\hat{\mathrm{U}}^{(\mathrm{m})}$ to the quantum state $\left|\psi^{(\mathrm{m})}\right\rangle$ defined in Eq.(3). The resulting quantum state can be expressed as [47]

$$\begin{aligned}\left|\psi'^{(\mathrm{m})}\right\rangle &= \hat{\mathrm{U}}^{(\mathrm{m})}\left|\psi^{(\mathrm{m})}\right\rangle = \hat{\mathrm{U}}^{(\mathrm{m})} f\left(\hat{a}_{\xi}^{\dagger(\mathrm{m})}\right)|0\rangle = \hat{\mathrm{U}}^{(\mathrm{m})} f\left(\hat{a}_{\xi}^{\dagger(\mathrm{m})}\right)\hat{\mathrm{U}}^{\dagger(\mathrm{m})}|0\rangle \\ &= f\left(\hat{\mathrm{U}}^{(\mathrm{m})}\hat{a}_{\xi}^{\dagger(\mathrm{m})}\hat{\mathrm{U}}^{\dagger(\mathrm{m})}\right)|0\rangle . \end{aligned} \tag{10}$$

Considering that the field transformation via this optical device is equivalent to the unitary transformation on quantum information as described in Eq.(8), we obtain

$$\left|\psi'^{(\mathrm{m})}\right\rangle = f\left(\sum_{i=0}^{d-1}\xi_i\hat{\mathrm{U}}^{(\mathrm{m})}\hat{a}_{m_i}^{\dagger}\hat{\mathrm{U}}^{\dagger(\mathrm{m})}\right)|0\rangle = f\left(\sum_{i=0}^{d-1}\xi_i'\,\hat{a}_{m_i}^{\dagger}\right)|0\rangle , \tag{11}$$

where the output probability amplitude ξ_i' of the i-th mode m_i is defined in Eq.(9). For further details, refer to Appendix A.

One should note that the operator $\hat{\mathrm{U}}$ is associated with the information transformation, while the operator $\hat{\mathrm{U}}^{(\mathrm{m})}$ transforms the quantum signal in the Fock space of mode m, which has an associated field operator $\hat{a}^{(\mathrm{m})}$. The field transformation matrix $\mathbf{U}^{(\mathrm{m})}$ has matrix elements that are identical to those of the quantum information transformation operator $\hat{\mathrm{U}}$, ensuring uniformity between the quantum signal and quantum information transformations

3. Frameworks for All-Quantum Mode Expansion, Reduction, and Mapping Operators

Thus far, we have presented the evolution of a quantum signal through an intra-mode unitary operator $\hat{\mathrm{U}}^{(\mathrm{m})}$ acting on the quantum state $\left|\psi^{(\mathrm{m})}\right\rangle$. Since this unitary operator keeps the signal's mode unchanged, it is referred to as intra-mode evolution.

This section focuses on the mathematical frameworks of three fundamental inter-mode operations: mode expansion, mode reduction, and mode mapping. This paper depicts the intra-mode unitary operator explained in section 2 by a square, and the mode mapper by a circle. Furthermore, the block diagrams for the mode expander and mode reducer are depicted as trapezoids, with the longer base oriented towards the larger space; the mode expander is rotated counter-clockwise by $\frac{\pi}{2}$, and the mode reducer is rotated clockwise by $-\frac{\pi}{2}$, see Fig. 3. The mode mapping operator $\hat{\mathrm{M}}^{(\mathrm{m})\to(\tilde{\mathrm{m}})}$ alters the physical realization of the quantum information by encoding the quantum information in mode $\tilde{\mathrm{m}}$ instead of mode m of the optical quantum signal. For instance, it can convert a polarization-encoded qubit into a time-encoded qubit. This process requires an inter-mode unitary operation, i.e., a polarization-to-time mode mapping. Also, the mode expansion module increases the dimensionality of the effective Hilbert space, enabling more flexibility for quantum operation. In contrast, the mode reduction module reduces the Hilbert space by discarding certain portions of the quantum information. These modules create a unified mathematical framework which not only deepens our understanding of quantum state of light and its manipulation, but also establishes a foundation for practical applications in quantum communications and computations.

3.1. Mode Expander (Inter-Mode Operation)

A mode expander increases the dimensionality of the input signal space by a factor of $\tilde{d}$, where $\tilde{d} \geq 2$. Mathematically speaking, the mode expansion operator $\hat{\mathrm{E}}^{(\mathrm{m})\to(\mathrm{m},\tilde{\mathrm{m}})}$ transforms a quantum signal $\left|\psi^{(\mathrm{m})}\right\rangle$, as described in Eq.(3), which has d discrete carriers of quantum information m_i for $0 \leq i < d$, into $\left|\psi_{\mathrm{E}}^{(\mathrm{m},\tilde{\mathrm{m}})}\right\rangle$ with $d_{\mathrm{e}} = d\tilde{d}$ carriers of quantum information $(m_i, \tilde{m}_j)$ for $0 \leq i < d$

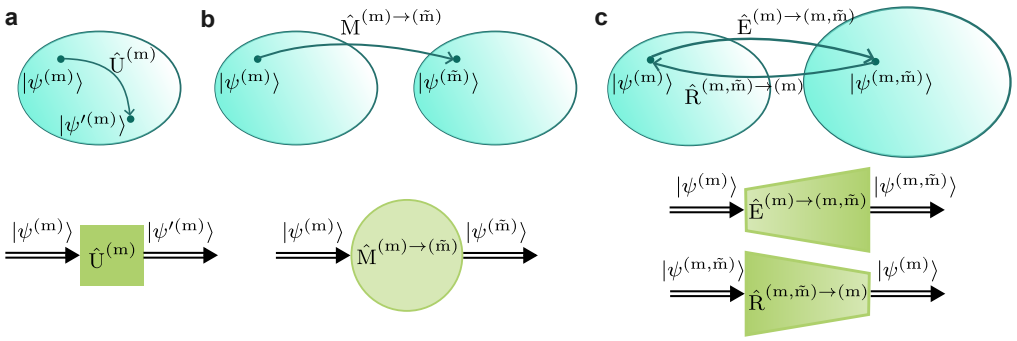

Fig. 3. Schematic diagram illustrating various modules within the signal space. **a** Unitary operator (intra-mode operation), **b** Mode mapping (inter-mode operation), **c** Mode expansion and reduction modules (inter-mode operations).

and $0 \leq j < \tilde{d}$. Assuming the input signal is in mode $\tilde{m}_0$, the transformation is expressible as follows

$$\begin{aligned}\left|\psi^{(\mathrm{m},\tilde{\mathrm{m}})}\right\rangle &= \left|\psi^{(\mathrm{m})}\right\rangle_{\tilde{m}_0} |0\rangle_{\tilde{m}_1} |0\rangle_{\tilde{m}_2} \ldots |0\rangle_{\tilde{m}_{\tilde{d}-1}} = \hat{\mathrm{E}}^{(\mathrm{m})\to(\mathrm{m},\tilde{\mathrm{m}})} \left|\psi^{(\mathrm{m})}\right\rangle = \hat{\mathrm{E}}^{(\mathrm{m})\to(\mathrm{m},\tilde{\mathrm{m}})} f\left(\hat{a}^{\dagger(\mathrm{m})}_{\xi}\right)|0\rangle \\ &= f\left(\hat{\mathrm{E}}^{(\mathrm{m})\to(\mathrm{m},\tilde{\mathrm{m}})} \hat{a}^{\dagger(\mathrm{m})}_{\xi} \hat{\mathrm{E}}^{\dagger(\mathrm{m})\to(\mathrm{m},\tilde{\mathrm{m}})}\right)|0\rangle = f\left(\hat{a}^{\dagger(\mathrm{m},\tilde{\mathrm{m}})}_{\xi}\right)|0\rangle\,, \end{aligned} \tag{12}$$

where

$$\hat{a}^{\dagger(\mathrm{m},\tilde{\mathrm{m}})}_{\xi} = \hat{\mathrm{E}}^{(\mathrm{m})\to(\mathrm{m},\tilde{\mathrm{m}})} \hat{a}^{\dagger(\mathrm{m})}_{\xi} \hat{\mathrm{E}}^{\dagger(\mathrm{m})\to(\mathrm{m},\tilde{\mathrm{m}})} = \sum_{i=0}^{d-1}\sum_{j=0}^{\tilde{d}-1} \xi_{i,j}\, \hat{a}^{\dagger}_{m_i,\tilde{m}_j}. \tag{13}$$

The last term in Eq.(13) is the generalization of Eq.(3) for two modes. Also, the coefficient $\xi_{i,j}$ represents the probability amplitude at mode $(m_i, \tilde{m}_j)$ in the expanded space, satisfying the normalization condition

$$\sum_{i=0}^{d-1}\sum_{j=0}^{\tilde{d}-1} |\xi_{i,j}|^2 = 1. \tag{14}$$

Also,

$$|\xi_i|^2 = \sum_{j=0}^{\tilde{d}-1} |\xi_{i,j}|^2. \tag{15}$$

For the case where the input signal is in the mode $\tilde{m}_0$ as shown in Eq.(12), Eq.(15) is simplified to

$$\xi_{i,j} = \xi_i\, \delta_{j,0}. \tag{16}$$

Moreover, one can deduce from Eq.(12) that

$$\hat{\mathrm{E}}^{\dagger(\mathrm{m})\to(\mathrm{m},\tilde{\mathrm{m}})} \hat{\mathrm{E}}^{(\mathrm{m})\to(\mathrm{m},\tilde{\mathrm{m}})} = \hat{\mathbb{1}}^{(\mathrm{m})}, \tag{17}$$

where the identity operator $\hat{\mathbb{1}}^{(\mathrm{m})}$ preserves the quantum signal's components at mode m. See Appendix B for further details.

3.1.1. Quantum Information Representation of the Mode Expansion Operator

Corresponding to the above mode expansion operator, one can introduce the expansion operator $\hat{\mathrm{E}}$ acting on the quantum information state of Eq.(1), $\left|\psi\right\rangle \in \mathcal{H}_d$. The operator $\hat{\mathrm{E}}$ can be expressed as a $d_{\mathrm{e}} \times d$ operator $\hat{\mathbb{1}} \otimes |u_0\rangle$, as follows [50]

$$\left|\psi_{\mathrm{E}}\right\rangle = \hat{\mathrm{E}}\left|\psi\right\rangle = \left(\hat{\mathbb{1}} \otimes |u_0\rangle\right)\left|\psi\right\rangle, \tag{18}$$

where $\hat{\mathbb{1}}$ denotes the $d \times d$ identity operator, and $|u_0\rangle$ is a $\tilde{d} \times 1$ column vector characterized by all elements being 0, except for the first element, which is 1, specifically

$$|u_0\rangle \equiv \begin{bmatrix} 1 & 0 & 0 & \dots & 0 \end{bmatrix}^{\top}. \tag{19}$$

The first element of the vector $|u_0\rangle$ in Eq.(19) corresponds to the mode $\tilde{m}_0$, whereas the remaining zero elements represent the newly introduced carriers of quantum information that may be employed in subsequent processes. It can be demonstrated that the expansion of the quantum information state in Eq.(1) gives (see Appendix B)

$$\left|\psi_{\mathrm{E}}\right\rangle = \hat{\mathrm{E}}\left|\psi\right\rangle = \sum_{i=0}^{d-1}\sum_{j=0}^{\tilde{d}-1} \xi_{i,j}\left|i\tilde{d}+j\right\rangle_L, \tag{20}$$

where similar to Eq.(16), we have $\xi_{i,j} = \xi_i\ \delta_{j,0}$. Considering the equation

$$\hat{\mathrm{E}}^{\dagger}\hat{\mathrm{E}} = (\hat{\mathbb{1}} \otimes \langle u_0|)(\hat{\mathbb{1}} \otimes |u_0\rangle) = \hat{\mathbb{1}} \otimes \langle u_0|u_0\rangle = \hat{\mathbb{1}}_{d\times d}, \tag{21}$$

the expansion operator $\hat{\mathrm{E}}$ acts as a $d_{\mathrm{e}} \times d$ Kraus operator.

Example I

Consider a time-bin encoded quantum signal, represented as

$$\left|\psi^{(\mathrm{t})}\right\rangle = f\left(\hat{a}_{\xi}^{\dagger(\mathrm{t})}\right)|0\rangle = f\left(\xi_0\hat{a}_{t_0}^{\dagger} + \xi_1\hat{a}_{t_1}^{\dagger}\right)|0\rangle, \tag{22}$$

where $|\xi_0|^2 + |\xi_1|^2 = 1$, entering path l_0 of a beam-splitter, as shown in Fig. 4-a. Given that the ground (vacuum) state exists in the input path l_1, it expands the dimension of the quantum state as follows

$$\left|\psi^{(\mathrm{t,l})}\right\rangle = \left|\psi^{(\mathrm{t})}\right\rangle_{l_0}|0\rangle_{l_1} = \hat{\mathrm{E}}^{(\mathrm{t})\to(\mathrm{t,l})}\left|\psi^{(\mathrm{t})}\right\rangle = f\left(\hat{a}_{\xi}^{\dagger(\mathrm{t,l})}\right)|0\rangle = f\left(\xi_0\hat{a}_{t_0,l_0}^{\dagger} + \xi_1\hat{a}_{t_1,l_0}^{\dagger}\right)|0\rangle. \tag{23}$$

In this scenario, the dimensional increase factor of the signal space is given by $\tilde{d} = 2$.

In the context of the quantum information description, applying the expansion operator defined in Eq.(18), specifically $\hat{\mathrm{E}} = \hat{\mathbb{1}} \otimes |u_0\rangle$, or its equivalent matrix representation, i.e.,

$$\mathbf{E} = \begin{bmatrix} 1 & 0 \\ 0 & 1 \end{bmatrix} \otimes \begin{bmatrix} 1 \\ 0 \end{bmatrix} = \begin{bmatrix} 1 & 0 & 0 & 0 \\ 0 & 0 & 1 & 0 \end{bmatrix}^{\mathrm{T}} \tag{24}$$

to the input vector

$$\left|\psi\right\rangle \equiv \begin{bmatrix} \xi_0 & \xi_1 \end{bmatrix}^{\mathrm{T}} \tag{25}$$

produces the output vector

$$\left|\psi_{\mathrm{E}}\right\rangle \equiv \begin{bmatrix} \xi_{0,0} & \xi_{0,1} & \xi_{1,0} & \xi_{1,1} \end{bmatrix}^{\mathrm{T}} = \begin{bmatrix} \xi_0 & 0 & \xi_1 & 0 \end{bmatrix}^{\mathrm{T}}. \tag{26}$$

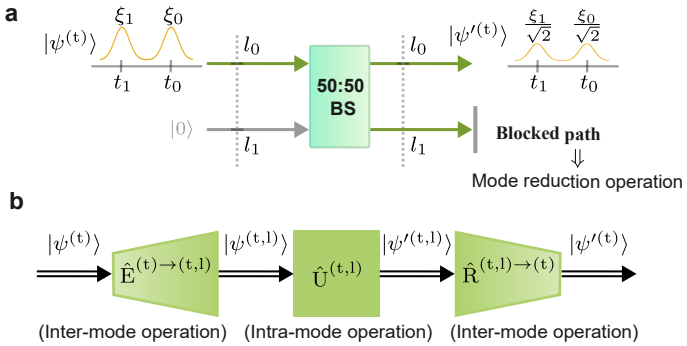

Fig. 4. An illustration of mode expansion, unitary operation, and mode reduction. **a** A time-bin encoded quantum state enters the beam splitter from port l_0 , representing mode expansion. Blocking the output port l_1 discards the information from this path, which is considered mode reduction. **b** Block diagram of the operation performed by the framework of Figure a.

3.1.2. Beam-Splitter Operator

Applying the operator of the 50 : 50 beam-splitter, denoted as $\hat{\mathrm{B}}^{(\mathrm{l})}$, which has the field transformation matrix

$$\mathbf{B}^{(\mathrm{l})} = \frac{1}{\sqrt{2}} \begin{bmatrix} 1 & 1 \\ 1 & -1 \end{bmatrix}, \tag{27}$$

to the path degree of the quantum state $\left|\psi^{(\mathrm{t,l})}\right\rangle$ results in

$$\begin{aligned} \left|\psi'^{(\mathrm{t,l})}\right\rangle &= \hat{\mathrm{U}}^{(\mathrm{t,l})} \left|\psi_{\mathrm{E}}^{(\mathrm{t,l})}\right\rangle = \left(\hat{\mathbb{1}}^{(\mathrm{t})} \otimes \hat{\mathrm{B}}^{(\mathrm{l})}\right) \left|\psi_{\mathrm{E}}^{(\mathrm{t,l})}\right\rangle = f\left[\left(\hat{\mathbb{1}}^{(\mathrm{t})} \otimes \hat{\mathrm{B}}^{(\mathrm{l})}\right) \hat{a}_{\xi}^{\dagger(\mathrm{t,l})} \left(\hat{\mathbb{1}}^{(\mathrm{t})} \otimes \hat{\mathrm{B}}^{\dagger(\mathrm{l})}\right)\right] |0\rangle \\ &= f\left(\frac{\xi_0 \hat{a}^{\dagger}_{t_0,l_0} + \xi_0 \hat{a}^{\dagger}_{t_0,l_1} + \xi_1 \hat{a}^{\dagger}_{t_1,l_0} + \xi_1 \hat{a}^{\dagger}_{t_1,l_1}}{\sqrt{2}}\right) |0\rangle , \end{aligned} \tag{28}$$

where similar equations as Eq.(10) and Eq.(11) are used. Additionally, the identity operator $\hat{\mathbb{1}}^{(\mathrm{t})}$ indicates that the temporal degree remains unaffected by the beam-splitter operator.

3.2. Mode Reducer (Inter-Mode Operation)

As opposed to the mode expander, the mode reduction module functions to eliminate a portion of signal's degree of freedom, reducing the dimensionality of the signal space by a factor of $1/\tilde{d}$ ($\tilde{d} \geq 2$). In the framework of the quantum signal description, a mode reduction operator $\hat{\mathrm{R}}_{\tilde{m}_{j_0}}^{(\mathrm{m},\tilde{\mathrm{m}})\to(\mathrm{m})}$ transforms the quantum signal with quantum state $\left|\psi^{(\mathrm{m},\tilde{\mathrm{m}})}\right\rangle$ which comprises d_{e} discrete modes $(m_i, \tilde{m}_j)$, for $0 \leq i < d$ and $0 \leq j < \tilde{d}$ as specified in Eq.(13), into $\left|\psi^{(\mathrm{m})}\right\rangle \equiv \left|\psi^{(\mathrm{m})}\right\rangle_{\tilde{m}_{j_0}}$. The subscript $\tilde{m}_{j_0}$ of the mode reduction operator $\hat{\mathrm{R}}_{\tilde{m}_{j_0}}$ highlights the mode component in which the state is projected. The notation $\left|\psi^{(\mathrm{m})}\right\rangle_{\tilde{m}_{j_0}}$ indicates that the quantum signal utilizes the mode (m) as carriers of quantum information, while the mode $\tilde{\mathrm{m}}$ is identical and equals to $\tilde{m}_{j_0}$ for all components of the quantum signal. Notably, since the $\tilde{m}_{j_0}$ mode is

identical across all components, it is typically omitted from the notation. To obtain the reduced state, one should take a partial trace over all modes excluding those with $\tilde{m}_J$ terms. Consequently, the reduced state can be expressed as follows

$$\rho^{(\mathrm{m})}_{\tilde{m}_{j_0}} = \hat{\mathrm{R}}^{(\mathrm{m},\tilde{\mathrm{m}})\to(\mathrm{m})}_{\tilde{m}_{j_0}} \rho^{(\mathrm{m},\tilde{\mathrm{m}})} \hat{\mathrm{R}}^{\dagger(\mathrm{m},\tilde{\mathrm{m}})\to(\mathrm{m})}_{\tilde{m}_{j_0}} = \mathrm{Tr}_{(m_I,\tilde{m}_J)\in\mathcal{T}} \left\{ \rho^{(\mathrm{m},\tilde{\mathrm{m}})} \right\}, \tag{29}$$

where $\rho^{(\mathrm{m},\tilde{\mathrm{m}})} = \left|\psi^{(\mathrm{m},\tilde{\mathrm{m}})}\right\rangle\!\left\langle\psi^{(\mathrm{m},\tilde{\mathrm{m}})}\right|$, and

$$\mathcal{T} = \left\{ (m_I, \tilde{m}_J) :\ 0 \le I < d,\ 0 \le J < \tilde{d}\ , J \ne j_0 \right\}. \tag{30}$$

The analysis of the transformation in Eq.(29) for general Fock state function f exceeds the focus of this paper. However, for the two prevalent quantum sources, including the single photon and the coherent light, which are widely employed in quantum key distribution and quantum secure direct communication, this analysis is straightforward. Furthermore, to quantify the quality of the mode reduction operation, we invert the mode expansion given in Eq.(12) using the mode reduction operation described in Eq.(29). Our desired quantum signal is the input of the hypothetical mode expander with signal mode m and common mode $\tilde{m}_{j_0}$, represented as

$$\left|\psi^{(\mathrm{m})}_{\mathrm{D}}\right\rangle_{\tilde{m}_{j_0}} = f\left(\hat{a}^{\dagger(\mathrm{m})}_{\xi'}\right)|0\rangle = f\left(\sum_{i=0}^{d-1} \frac{\xi_{i,j_0}}{\tilde{\xi}_{j_0}} \hat{a}^{\dagger}_{m_i,\tilde{m}_{j_0}}\right)|0\rangle\,. \tag{31}$$

In Eq.(31), the subscript D indicates the desired state, and the normalization factor $\tilde{\xi}_{j_0}$ is defined as

$$\tilde{\xi}_{j_0} = \left(\sum_{i=0}^{d-1} |\xi_{i,j_0}|^2\right)^{1/2}. \tag{32}$$

We then compare the mode reducer's output signal with the desired signal from Eq.(31) by utilizing the attenuation factor for the coherent light and the success probability for the single photon state as quality metrics.

For the coherent state of light with complex amplitude α, Eq.(29) can be reduced to (see Appendix C.1)

$$\left|\psi^{(\mathrm{m})}\right\rangle_{\tilde{m}_{j_0}} = \hat{\mathrm{R}}^{(\mathrm{m},\tilde{\mathrm{m}})\to(\mathrm{m})}_{\tilde{m}_{j_0}} \left|\psi^{(\mathrm{m},\tilde{\mathrm{m}})}\right\rangle = f_{\alpha\tilde{\xi}_{j_0}}\left(\sum_{i=0}^{d-1} \frac{\xi_{i,j_0}}{\tilde{\xi}_{j_0}} \hat{a}^{\dagger}_{m_i,\tilde{m}_{j_0}}\right)|0\rangle = \prod_{i=0}^{d-1} \left|\alpha\ \xi_{i,j_0}\right\rangle_{m_i,\tilde{m}_{j_0}}. \tag{33}$$

By discarding the common mode component $\tilde{m}_{j_0}$, Eq.(33) becomes

$$\left|\psi^{(\mathrm{m})}\right\rangle \equiv \left|\psi^{(\mathrm{m})}\right\rangle_{\tilde{m}_{j_0}} = \prod_{i=0}^{d-1} \left|\alpha\ \xi_{i,j_0}\right\rangle_{m_i} = f_{\alpha\tilde{\xi}_{j_0}}\left(\hat{a}^{\dagger(\mathrm{m})}_{\xi'}\right)|0\rangle\,, \tag{34}$$

where the subscript of f denotes the complex amplitude of the state, and the mean photon number (intensity) decreases from $|\alpha|^2$ to $|\alpha\tilde{\xi}_{j_0}|^2$, leading to an attenuation factor of $|\tilde{\xi}_{j_0}|^2$. Also,

$$\hat{a}^{\dagger(\mathrm{m})}_{\xi'} = \sum_{i=0}^{d-1} \frac{\xi_{i,j_0}}{\tilde{\xi}_{j_0}}\ \hat{a}^{\dagger}_{m_i}. \tag{35}$$

For the single photon state, as derived in Appendix C.2, the output state of Eq.(29) is represented as

$$\rho^{(\mathrm{m})}_{\tilde{m}_{j_0}} = \sum_{i,i'} \xi_{i,j_0}\xi^{*}_{i',j_0}\hat{a}^{\dagger}_{m_i,\tilde{m}_{j_0}} \left|0\right\rangle\!\left\langle 0\right| \hat{a}_{m_{i'},\tilde{m}_{j_0}} + \sum_{i=0}^{d-1}\sum_{\substack{j=0\\ j\neq j_0}}^{\tilde{d}-1} |\xi_{i,j}|^2 \left|0\right\rangle\!\left\langle 0\right| . \tag{36}$$

Equation (36) demonstrates that a single photon can be detected in the desired mode j_0 with a probability of $p = |\tilde{\xi}_{j_0}|^2$, see Eq.(C.21). Conversely, there is a probability of $1 - p$ that the output will yield a vacuum state $|0\rangle$, which is not suitable for transmitting quantum information. The vacuum state associated with the lost photon is disregarded; however, its trace is retained through the operation's success probability The success probability is defined as the likelihood of observing a single photon in mode $\tilde{m}_{j_0}$. By this definition, Eq.(29) is simplified to (see Appendix C.2)

$$\left|\psi^{(\mathrm{m})}\right\rangle_{\tilde{m}_{j_0}} = \hat{\mathrm{R}}^{(\mathrm{m},\tilde{\mathrm{m}})\to(\mathrm{m})}_{\tilde{m}_{j_0}} \left|\psi^{(\mathrm{m},\tilde{\mathrm{m}})}\right\rangle = \sum_{i=0}^{d-1} \frac{\xi_{i,j_0}}{\tilde{\xi}_{j_0}} \hat{a}^{\dagger}_{m_i,\tilde{m}_{j_0}} |0\rangle . \tag{37}$$

Dropping the common mode $\tilde{m}_{j_0}$ from Eq.(37) gives

$$\left|\psi^{(\mathrm{m})}\right\rangle = \hat{\mathrm{R}}^{(\mathrm{m},\tilde{\mathrm{m}})\to(\mathrm{m})}_{\tilde{m}_{j_0}} \left|\psi^{(\mathrm{m},\tilde{\mathrm{m}})}\right\rangle = \sum_{i=0}^{d-1} \frac{\xi_{i,j_0}}{\tilde{\xi}_{j_0}} \hat{a}^{\dagger}_{m_i} |0\rangle = f\left(\sum_{i=0}^{d-1} \frac{\xi_{i,j_0}}{\tilde{\xi}_{j_0}} \hat{a}^{\dagger}_{m_i}\right)|0\rangle = f\left(\hat{a}^{\dagger(\mathrm{m})}_{\xi'}\right)|0\rangle , \tag{38}$$

where Eq.(35) is used. Also, the success probability of the reduced state of a single photon source is given by $\mathcal{S} = p = |\tilde{\xi}_{j_0}|^2$, as indicated in Eq.(C.22), respectively.

Form Eq.(34) and Eq.(38), it is concluded that the mode reducer affects both single photon and coherent states in a similar manner. The only distance is the fact that for coherent states, the intensity is diminished by the factor $|\tilde{\xi}_{j_0}|^2$, while for single photons, the success probability is reduced by the same factor $|\tilde{\xi}_{j_0}|^2$. Consequently, the success probability for a single photon input corresponds to the intensity attenuation factor for a coherent state input. As a result, we denote both using the parameter

$$\mathcal{S} = |\tilde{\xi}_{j_0}|^2 \equiv 10\log_{10}\left(|\tilde{\xi}_{j_0}|^2\right) \text{ dB}. \tag{39}$$

Additionally, in the remainder of this paper, to facilitate the simultaneous analysis of single photon and coherent states, we omit the amplitude α from the subscript of the coherent function f_α, and simply refer to it as f. However, this function is associated with the attenuation factor (success probability) $\mathcal{S}$. Consequently, the mode reduction procedure for both the single photon and coherent states can be stated as follows

$$\left|\psi^{(\mathrm{m})}\right\rangle = \hat{\mathrm{R}}^{(\mathrm{m},\tilde{\mathrm{m}})\to(\mathrm{m})}_{\tilde{m}_{j_0}} \left|\psi^{(\mathrm{m},\tilde{\mathrm{m}})}\right\rangle = f\left(\hat{a}^{\dagger(\mathrm{m})}_{\xi'}\right)|0\rangle = f\left(\sum_{i=0}^{d-1} \frac{\xi_{i,j_0}}{\tilde{\xi}_{j_0}} \hat{a}^{\dagger}_{m_i}\right)|0\rangle , \tag{40}$$

with success probability $\mathcal{S} = |\tilde{\xi}_{j_0}|^2$. In the following, two examples are presented to clarify Eq.(34) and Eq.(38).

Example II: Coherent state

In Fig. 4, consider the case where the input is a coherent light with intensity (mean photon number) $|\alpha|^2$. The output state has components on both the time and path modes, as described

by Eq.(28), and can be expressed as follows

$$\left|\psi'^{(\mathrm{t,l})}\right\rangle = f_{\alpha}\left(\frac{\xi_0\hat{a}^{\dagger}_{t_0,l_0}+\xi_0\hat{a}^{\dagger}_{t_0,l_1}+\xi_1\hat{a}^{\dagger}_{t_1,l_0}+\xi_1\hat{a}^{\dagger}_{t_1,l_1}}{\sqrt{2}}\right)|0\rangle$$
$$= \left|\frac{\alpha\xi_0}{\sqrt{2}}\right\rangle_{t_0,l_0}\left|\frac{\alpha\xi_0}{\sqrt{2}}\right\rangle_{t_0,l_1}\left|\frac{\alpha\xi_1}{\sqrt{2}}\right\rangle_{t_1,l_0}\left|\frac{\alpha\xi_1}{\sqrt{2}}\right\rangle_{t_1,l_1}. \tag{41}$$

If the line $j = 1$ (l_1) is blocked, the output is associated with line $j_0 = 0$ (l_0). Therefore, from Eq.(33), the state of the system will change as follows

$$\left|\psi'^{(\mathrm{t})}\right\rangle_{l_0} = \hat{\mathrm{R}}^{(\mathrm{t,l})\to(\mathrm{t})}_{l_0}\left|\psi'^{(\mathrm{t,l})}\right\rangle = \left|\frac{\alpha\xi_0}{\sqrt{2}}\right\rangle_{t_0,l_0}\left|\frac{\alpha\xi_1}{\sqrt{2}}\right\rangle_{t_1,l_0}. \tag{42}$$

By disregarding the trivial mode l_0, Eq.(42) is simplified according to Eq.(34) as

$$\left|\psi'^{(\mathrm{t})}\right\rangle = \left|\frac{\alpha\xi_0}{\sqrt{2}}\right\rangle_{t_0}\left|\frac{\alpha\xi_1}{\sqrt{2}}\right\rangle_{t_1} = f_{\frac{\alpha}{\sqrt{2}}}\left(\xi_0\hat{a}^{\dagger}_{t_0}+\xi_1\hat{a}^{\dagger}_{t_1}\right)|0\rangle = f_{\frac{\alpha}{\sqrt{2}}}\left(\hat{a}^{\dagger(\mathrm{t})}_{\xi'}\right)|0\rangle, \tag{43}$$

where the mean photon number decreases from $|\alpha|^2$ to $\frac{|\alpha|^2}{2}$, resulting in the attenuation factor of $\mathcal{S} = \left(\frac{1}{\sqrt{2}}\right)^2 = 0.5 \equiv -3\mathrm{dB}$. Additionally, we have

$$\hat{a}^{\dagger(\mathrm{t})}_{\xi'} = \xi_0\hat{a}^{\dagger}_{t_0} + \xi_1\hat{a}^{\dagger}_{t_1}. \tag{44}$$

Example III: Single photon state

As a second example, let us consider another scenario of Fig. 4, where the input is a single photon light. Therefore, the Fock function is $f(\hat{a}^{\dagger}_{\xi}) = \hat{a}^{\dagger}_{\xi}$, and $\left|\psi'^{(\mathrm{t,l})}\right\rangle$ can be expressed as follows

$$\left|\psi'^{(\mathrm{t,l})}\right\rangle = \left(\frac{\xi_0\hat{a}^{\dagger}_{t_0,l_0}+\xi_0\hat{a}^{\dagger}_{t_0,l_1}+\xi_1\hat{a}^{\dagger}_{t_1,l_0}+\xi_1\hat{a}^{\dagger}_{t_1,l_1}}{\sqrt{2}}\right)|0\rangle$$
$$= \frac{\xi_0}{\sqrt{2}}|1\rangle_{t_0,l_0}|0\rangle_{t_0,l_1}|0\rangle_{t_1,l_0}|0\rangle_{t_1,l_1} + \frac{\xi_0}{\sqrt{2}}|0\rangle_{t_0,l_0}|1\rangle_{t_0,l_1}|0\rangle_{t_1,l_0}|0\rangle_{t_1,l_1}$$
$$+ \frac{\xi_1}{\sqrt{2}}|0\rangle_{t_0,l_0}|0\rangle_{t_0,l_1}|1\rangle_{t_1,l_0}|0\rangle_{t_1,l_1} + \frac{\xi_1}{\sqrt{2}}|0\rangle_{t_0,l_0}|0\rangle_{t_0,l_1}|0\rangle_{t_1,l_0}|1\rangle_{t_1,l_1}. \tag{45}$$

If line l_1 is blocked, resulting in output line $j_0 = 0$ corresponding to the first and third terms in Eq.(45), the system's state will change according to Eq.(37) as follows

$$\left|\psi'^{(\mathrm{t})}\right\rangle_{l_0} = \xi_0|1\rangle_{t_0,l_0}|0\rangle_{t_1,l_0} + \xi_1|0\rangle_{t_0,l_0}|1\rangle_{t_1,l_0} = \xi_0\hat{a}^{\dagger}_{t_0,l_0}|0\rangle + \xi_1\hat{a}^{\dagger}_{t_1,l_0}|0\rangle, \tag{46}$$

where the normalization factor using Eq.(32) is

$$\tilde{\xi}_0 = \sqrt{\left|\frac{\xi_0}{\sqrt{2}}\right|^2 + \left|\frac{\xi_1}{\sqrt{2}}\right|^2} = \frac{1}{\sqrt{2}}. \tag{47}$$

By neglecting the trivial mode l_0, Eq.(46) is simplified to

$$\left|\psi'^{(\mathrm{t})}\right\rangle = \xi_0|1\rangle_{t_0}|0\rangle_{t_1} + \xi_1|0\rangle_{t_0}|1\rangle_{t_1} = \xi_0\hat{a}^{\dagger}_{t_0}|0\rangle + \xi_1\hat{a}^{\dagger}_{t_1}|0\rangle = f\left(\hat{a}^{\dagger(\mathrm{t})}_{\xi'}\right)|0\rangle, \tag{48}$$

where $\hat{a}^{\dagger(\mathrm{t})}_{\xi'}$ is defined in Eq.(44), and the success probability is $\mathcal{S} = \left(\frac{1}{\sqrt{2}}\right)^2 = 0.5 \equiv -3\mathrm{dB}$.

3.2.1. Quantum Information Representation of the Mode Reduction Operator

Corresponding to the aforementioned mode reduction operator, it is possible to introduce the information representation of the reduction operator $\hat{\mathrm{R}}_{j_0}$ for a designated index $j_0 \in \{0, 1, ...\tilde{d}-1\}$, which acts on the quantum information state $\left|\psi\right\rangle \in \mathcal{H}_{d_\mathrm{e}}$, expressed as

$$\left|\psi\right\rangle = \sum_{i=0}^{d-1}\sum_{j=0}^{\tilde{d}-1} \xi_{i,j} \left|i\tilde{d}+j\right\rangle_L . \tag{49}$$

The mode reduction operator transforms the effective Hilbert space from $\mathcal{H}_{d_\mathrm{e}}$ to $\mathcal{H}_d$, where $d_\mathrm{e} = d\tilde{d}$. To characterize a quantum information processor capable of reducing the dimensionality of the quantum state in Eq.(49), it is essential to reformulate it in the following form

$$\left|\psi\right\rangle = \sum_{i=0}^{d-1}\sum_{j=0}^{\tilde{d}-1} \xi_{i,j} \left|i\right\rangle_{L_1} \left|j\right\rangle_{L_2} , \tag{50}$$

where $\left|i\right\rangle_{L_1}$ and $\left|j\right\rangle_{L_2}$ denote the i-th and j-th logical basis state within the Hilbert spaces $\mathcal{H}_d$ and $\mathcal{H}_{\tilde{d}}$, respectively. These states satisfy the relation $\left|i\tilde{d}+j\right\rangle_L = \left|i\right\rangle_{L_1}\left|j\right\rangle_{L_2}$. Consequently, the operator $\hat{\mathrm{R}}_{j_0}$ can be expressed as

$$\left|\psi_\mathrm{R}\right\rangle_{j_0} = \hat{\mathrm{R}}_{j_0}\left|\psi\right\rangle = \frac{\left(\hat{\mathbb{1}}\otimes\left\langle j_0\right|\right)\left|\psi\right\rangle}{\left\|\left(\hat{\mathbb{1}}\otimes\left\langle j_0\right|\right)\left|\psi\right\rangle\right\|} = \frac{1}{\tilde{\xi}_{j_0}}\left(\hat{\mathbb{1}}\otimes\left\langle j_0\right|\right)\left|\psi\right\rangle , \tag{51}$$

where $\hat{\mathbb{1}}$ denotes the $d\times d$ identity operator, and $\left\langle j_0\right|$ is a $1\times\tilde{d}$ row vector characterized by all elements being zero, except for the j_0-th element. Additionally, $\tilde{\xi}_{j_0}$ is the normalization coefficient defined in Eq.(32). In fact, Eq.(51) describes the mode reduction operator as a $d\times d_\mathrm{e}$ operator $\hat{\mathbb{1}}\otimes\left\langle j_0\right|$ (compare this with the mode expansion operator in Eq.(18)). Due to the loss of some information during the mode reduction process, the norm of the resulting state decreases from 1 to $|\tilde{\xi}_{j_0}|^2$, which is compensated by the normalization coefficient $\frac{1}{\tilde{\xi}_{j_0}}$, depending on the coefficients of the input state $\left|\psi\right\rangle$. Substituting Eq.(50) into Eq.(51) yields

$$\left|\psi_\mathrm{R}\right\rangle_{j_0} = \hat{\mathrm{R}}_{j_0}\left|\psi\right\rangle = \frac{1}{\tilde{\xi}_{j_0}}\sum_{i=0}^{d-1}\sum_{j=0}^{\tilde{d}-1}\xi_{i,j}\left(\hat{\mathbb{1}}\left|i\right\rangle\right)_{L_1}\otimes\left(\left\langle j_0|j\right\rangle\right)_{L_2} = \sum_{i=0}^{d-1}\frac{\xi_{i,j_0}}{\tilde{\xi}_{j_0}}\left|i\right\rangle_{L_1} \equiv \sum_{i=0}^{d-1}\frac{\xi_{i,j_0}}{\tilde{\xi}_{j_0}}\left|i\tilde{d}+j_0\right\rangle_L . \tag{52}$$

The last term in Eq.(52) arises from the fact that the constant state $\left|j_0\right\rangle_{L_2}$ does not convey any information, which leads to $\left|i\right\rangle_{L_1} \equiv \left|i\right\rangle_{L_1}\left|j_0\right\rangle_{L_2} = \left|i\tilde{d}+j_0\right\rangle_L$.

The quality of the mode reduction informational operator $\hat{\mathrm{R}}_{j_0}$ is determined by the fidelity between the reduced quantum information state $\left|\psi_\mathrm{R}\right\rangle_{j_0}$ calculated in Eq.(52) and the quantum information representation of the desired state described in Eq.(31), denoted as $\left|\psi_\mathrm{D}\right\rangle_{j_0}$. The fidelity between two arbitrary pure states $\left|\psi\right\rangle$ and $\left|\phi\right\rangle$ is defined as [22, 51]

$$\mathcal{F}(\left|\psi\right\rangle, \left|\phi\right\rangle) = \left|\left\langle\psi|\phi\right\rangle\right| . \tag{53}$$

Therefore, the fidelity parameter between $\left|\psi_{\mathrm{R}}\right\rangle_{j_0}$ and $\left|\psi_{\mathrm{D}}\right\rangle_{j_0}$ is calculated as follows

$$\mathcal{F}(\left|\psi_{\mathrm{D}}\right\rangle_{j_0}, \left|\psi_{\mathrm{R}}\right\rangle_{j_0}) = \left|{}_{j_0}\!\left\langle\psi_{\mathrm{D}}\right|\left.\psi_{\mathrm{R}}\right\rangle_{j_0}\right| = \left|\sum_{i,i'=0}^{d-1} \frac{\xi_{i,j_0}\ \xi^{*}_{i',j_0}}{|\tilde{\xi}_{j_0}|^2}\ \delta_{i,i'}\right| = \frac{\sum_{i=0}^{d-1}|\xi_{i,j_0}|^2}{|\tilde{\xi}_{j_0}|^2} = 1, \tag{54}$$

where Eq.(31), Eq.(52), and the orthonormality of logical basis states are utilized. Consequently, regardless of the physical realization of the quantum state, the fidelity of mode reduction in the quantum information representation is equal to 1.

3.3. Mode Mapper (Inter-Mode → Intra-Mode → Inter-Mode Operation)

A mode mapping module transfers the quantum information encoded in mode m into mode $\tilde{\mathrm{m}}$. From a mathematical perspective, a mode mapping operator $\hat{\mathrm{M}}^{(\mathrm{m})\to(\tilde{\mathrm{m}})}$ takes a quantum signal $\left|\psi^{(\mathrm{m})}\right\rangle$ characterized by d discrete carriers of quantum information m_i for $0 \le i < d$, as defined in Eq.(3), and converts it into $\left|\psi^{(\tilde{\mathrm{m}})}\right\rangle$ with $\tilde{d} = d$ discrete modes $\tilde{m}_i$. This transformation can be expressed mathematically as follows

$$\left|\psi^{(\tilde{\mathrm{m}})}\right\rangle = \hat{\mathrm{M}}^{(\mathrm{m})\to(\tilde{\mathrm{m}})}\left|\psi^{(\mathrm{m})}\right\rangle = f\left(\sum_{i=0}^{d-1}\xi_i\hat{a}^{\dagger}_{\tilde{m}_i}\right)|0\rangle\,, \tag{55}$$

where ξ_i denotes the probability amplitude associated with the mode m_i in $\left|\psi^{(\mathrm{m})}\right\rangle$ and mode $\tilde{m}_i$ in $\left|\psi^{(\tilde{\mathrm{m}})}\right\rangle$. Indeed, a mode mapping operator $\hat{\mathrm{M}}^{(\mathrm{m})\to(\tilde{\mathrm{m}})}$ alters the physical state (signal) of quantum light while retaining its quantum information content. Specifically, the mode mapping operator performs the following transformations

$$\begin{cases} \hat{a}^{\dagger}_{m_0,\tilde{m}_0} \longrightarrow \hat{a}^{\dagger}_{m_{i_0},\tilde{m}_0} \\ \hat{a}^{\dagger}_{m_1,\tilde{m}_0} \longrightarrow \hat{a}^{\dagger}_{m_{i_0},\tilde{m}_1} \\ \hat{a}^{\dagger}_{m_2,\tilde{m}_0} \longrightarrow \hat{a}^{\dagger}_{m_{i_0},\tilde{m}_2} \\ \qquad\vdots \\ \hat{a}^{\dagger}_{m_{d-1},\tilde{m}_0} \longrightarrow \hat{a}^{\dagger}_{m_{i_0},\tilde{m}_{d-1}} \end{cases}, \tag{56}$$

where i_0 is an element of the set $\{0, 1, 2, \ldots, d-1\}$. As an example, the mode mapping operation can be realized as a combination of mode expansion, followed by a unitary operation in the extended space, and subsequently a mode reduction, expressed as

$$\left|\psi^{(\tilde{\mathrm{m}})}\right\rangle = \hat{\mathrm{M}}^{(\mathrm{m})\to(\tilde{\mathrm{m}})}\left|\psi^{(\mathrm{m})}\right\rangle = \hat{\mathrm{R}}^{(\mathrm{m},\tilde{\mathrm{m}})\to(\tilde{\mathrm{m}})}_{m_{i_0}}\hat{\mathrm{U}}^{(\mathrm{m},\tilde{\mathrm{m}})}\left(\hat{\mathrm{E}}^{(\mathrm{m})\to(\mathrm{m},\tilde{\mathrm{m}})}\left|\psi^{(\mathrm{m})}\right\rangle\right). \tag{57}$$

Each mode mapping operator functions as an identity operator in the quantum information's Hilbert space $\mathcal{H}_d$, which is expressed as

$$\hat{\mathrm{M}} = \hat{\mathbb{1}}_{d\times d}. \tag{58}$$

4. Comparative Analysis of All-Quantum Mode Mapping Structures

In this section, we present a comparative analysis of various all-quantum mode mapping structures commonly used in quantum communications. These structures play a critical role in passing

quantum information across different quantum communication's node, and we will evaluate their characteristics by calculating the fidelity and success probability of each mode mapping module. It is assumed that the optical devices employed are ideal, disregarding any photon losses and imperfections associated with these devices. All these mode mapping operators function as identity operators $\hat{\mathbb{1}}$ within the d-dimensional Hilbert space, as discussed in Section 3.3. Consequently, the subsequent discussion will focus only on the signal description of the mode mapping modules.

4.1. *Path-to-Time Mode Mapping via Beam-Splitter*

Consider the quantum information is encoded in the path lines of a quantum signal, represented as follows

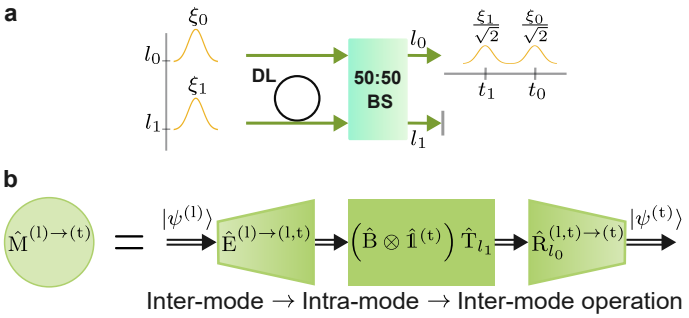

Fig. 5. Path-to-time mode mapper via beam-splitter with $\mathcal{F} = 1$ and $\mathcal{S} = 0.5$. DL: delay line; BS: beam-splitter.

$$\left|\psi^{(\mathrm{l})}\right\rangle = f\left(\hat{a}_{\xi}^{\dagger(\mathrm{l})}\right)|0\rangle = f\left(\xi_0\hat{a}_{l_0}^{\dagger} + \xi_1\hat{a}_{l_1}^{\dagger}\right)|0\rangle\,, \tag{59}$$

where the coefficients satisfy the normalization condition $|\xi_0|^2 + |\xi_1|^2 = 1$. Figure 5 represents a path-to-time mode mapping block which includes a delay line and a beam-splitter. Initially, the delay line operator $\hat{\mathrm{T}}_{l_1}$ on path line l_1 modifies the creation operators as follows

$$\begin{cases} \hat{a}_{l_0,t_0}^{\dagger} \to \hat{a}_{l_0,t_0}^{\dagger} \\ \hat{a}_{l_1,t_0}^{\dagger} \to \hat{a}_{l_1,t_1}^{\dagger}. \end{cases} \tag{60}$$

In essence, the delay line within this configuration implicitly includes a mode expansion operator $\hat{\mathrm{E}}^{(\mathrm{l})\to(\mathrm{l,t})}$, which expands the space from (l) to (l, t). The delay line operates in the expanded space as demonstrated by Eq.(60). Subsequently, the beam splitter utilizes the operator $\hat{\mathrm{B}}^{(\mathrm{l})}$ on the path modes while maintaining the temporal modes unchanged, resulting in

$$\begin{aligned}\left|\psi'^{(\mathrm{l,t})}\right\rangle &= \left(\hat{\mathrm{B}}^{(\mathrm{l})}\otimes\hat{\mathbb{1}}^{(\mathrm{t})}\right) f\left(\xi_0\hat{a}_{l_0,t_0}^{\dagger} + \xi_1\hat{a}_{l_1,t_1}^{\dagger}\right)|0\rangle = f\left(\frac{\xi_0\hat{a}_{l_0,t_0}^{\dagger} + \xi_0\hat{a}_{l_1,t_0}^{\dagger} + \xi_1\hat{a}_{l_0,t_1}^{\dagger} - \xi_1\hat{a}_{l_1,t_1}^{\dagger}}{\sqrt{2}}\right)|0\rangle \\ &= f\left(\hat{a}_{\xi'}^{\dagger(\mathrm{l,t})}\right), \end{aligned} \tag{61}$$

where Eq.(A.5), Eq.(A.7) and Eq.(27) are used.

Now, line l_1 is blocked, and according to section 3.2, the reduced quantum state is expressible as

$$\left|\psi^{(\mathrm{t})}\right\rangle_{l_0} = \hat{\mathrm{R}}_{l_0}^{(\mathrm{l,t})\to(\mathrm{t})}\left|\psi'^{(\mathrm{l,t})}\right\rangle = f\left(\xi_0\hat{a}_{l_0,t_0}^{\dagger} + \xi_1\hat{a}_{l_0,t_1}^{\dagger}\right)|0\rangle\,, \tag{62}$$

with $\mathcal{S} = \left(\frac{1}{\sqrt{2}}\right)^2 = 0.5$ for the single photon source, which corresponds to an intensity attenuation factor of 0.5 for the coherent state input. One can drop the unchanged, trivial mode l_0, which gives

$$\left|\psi^{(\mathrm{t})}\right\rangle = f\left(\hat{a}_{\xi}^{\dagger(\mathrm{t})}\right)|0\rangle = f\left(\xi_0\hat{a}_{t_0}^{\dagger} + \xi_1\hat{a}_{t_1}^{\dagger}\right)|0\rangle\,. \tag{63}$$

Comparing Eq.(59) and Eq.(63) yields

$$\begin{aligned}\left|\psi^{(\mathrm{t})}\right\rangle &= \hat{\mathrm{M}}^{(\mathrm{l})\to(\mathrm{t})}\left|\psi^{(\mathrm{l})}\right\rangle = \hat{\mathrm{M}}^{(\mathrm{l})\to(\mathrm{t})} f\left(\hat{a}_{\xi}^{\dagger(\mathrm{l})}\right)|0\rangle \\ &= \left[\hat{\mathrm{R}}_{l_0}^{(\mathrm{l,t})\to(\mathrm{t})}\left(\hat{\mathrm{B}}^{(\mathrm{l})}\otimes\hat{\mathbb{1}}^{(\mathrm{t})}\right)\hat{\mathrm{T}}_{l_1}\hat{\mathrm{E}}^{(\mathrm{l})\to(\mathrm{l,t})}\right] f\left(\hat{a}_{\xi}^{\dagger(\mathrm{l})}\right)|0\rangle = f\left(\hat{a}_{\xi}^{\dagger(\mathrm{t})}\right)|0\rangle\,.\end{aligned} \tag{64}$$

Thus, the mode mapping operator transforms $\hat{a}_{l_0}^{\dagger} \to \hat{a}_{t_0}^{\dagger}$ and $\hat{a}_{l_1}^{\dagger} \to \hat{a}_{t_1}^{\dagger}$ with fidelity $\mathcal{F} = 1$ and success probability $\mathcal{S} = 0.5$. This path-to-time mode mapping is extensively utilized in the transmitter of time-bin QKD employing asymmetric Mach-Zehnder interferometer structures [24, 52].

4.2. Time-to-Path Mode Mapping

Consider a time-encoded quantum state represented as follows

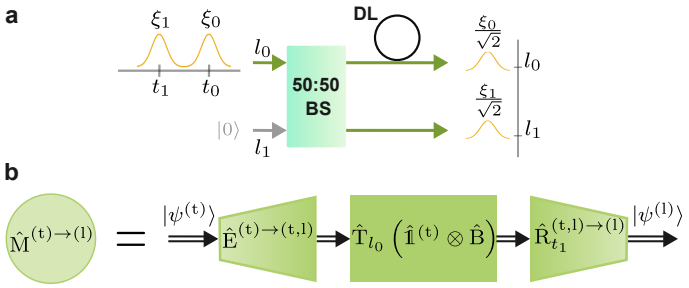

Fig. 6. Time-to-path mode mapper with $\mathcal{F} = 1$ and $\mathcal{S} = 0.5$. DL: delay line; BS: beam-splitter.

$$\left|\psi^{(\mathrm{t})}\right\rangle = f\left(\hat{a}_{\xi}^{\dagger(\mathrm{t})}\right)|0\rangle = f\left(\xi_0\hat{a}_{t_0}^{\dagger} + \xi_1\hat{a}_{t_1}^{\dagger}\right)|0\rangle\,. \tag{65}$$

Figure 6 illustrates a time-to-path mode mapping mechanism, which comprises a beam splitter followed by a delay line. The state $\left|\psi^{(\mathrm{t})}\right\rangle$ enters through line l_0 while port l_1 is in the vacuum ground state $|0\rangle$, functioning as a path mode expander. This can be expressed as

$$\left|\psi^{(\mathrm{t,l})}\right\rangle = \hat{\mathrm{E}}^{(\mathrm{t})\to(\mathrm{t,l})}\left|\psi^{(\mathrm{t})}\right\rangle = \left|\psi^{(\mathrm{t})}\right\rangle_{l_0}|0\rangle_{l_1} = f\left(\hat{a}_{\xi}^{\dagger(\mathrm{t,l})}\right)|0\rangle = f\left(\xi_0\hat{a}_{t_0,l_0}^{\dagger} + \xi_1\hat{a}_{t_1,l_0}^{\dagger}\right)|0\rangle\,, \tag{66}$$

where Eq.(23) is utilized. According to Eq.(28), the output state of the beam-splitter can be represented as

$$\begin{aligned}\left|\psi'^{(\mathrm{t,l})}\right\rangle &= \left(\hat{\mathbb{1}}^{(\mathrm{t})}\otimes\hat{\mathrm{B}}^{(\mathrm{l})}\right)\left|\psi^{(\mathrm{t,l})}\right\rangle = \left(\hat{\mathbb{1}}^{(\mathrm{t})}\otimes\hat{\mathrm{B}}^{(\mathrm{l})}\right) f\left(\hat{a}_{\xi}^{\dagger(\mathrm{t,l})}\right)|0\rangle \\ &= f\left(\frac{\xi_0\hat{a}_{t_0,l_0}^{\dagger} + \xi_0\hat{a}_{t_0,l_1}^{\dagger} + \xi_1\hat{a}_{t_1,l_0}^{\dagger} + \xi_1\hat{a}_{t_1,l_1}^{\dagger}}{\sqrt{2}}\right)|0\rangle\,.\end{aligned} \tag{67}$$

Subsequently, the delay line $\hat{\mathrm{T}}_{l_0}$ on path l_0 converts

$$\begin{cases} \hat{a}^{\dagger}_{t_0,l_0} \rightarrow \hat{a}^{\dagger}_{t_1,l_0} \\ \hat{a}^{\dagger}_{t_1,l_0} \rightarrow \hat{a}^{\dagger}_{t_2,l_0}. \end{cases} \tag{68}$$

Therefore, the quantum state after the delay line is expressible as

$$\left|\psi''^{(\mathrm{t,l})}\right\rangle = \hat{\mathrm{T}}_{l_0}\left|\psi'^{(\mathrm{t,l})}\right\rangle = f\left(\frac{\xi_0\hat{a}^{\dagger}_{t_1,l_0} + \xi_0\hat{a}^{\dagger}_{t_0,l_1} + \xi_1\hat{a}^{\dagger}_{t_2,l_0} + \xi_1\hat{a}^{\dagger}_{t_1,l_1}}{\sqrt{2}}\right)|0\rangle\,. \tag{69}$$

One can disregard the temporal components t_0 and t_2 and focus solely on the information contained in mode t_1, utilizing mode reduction operation as follows

$$\left|\psi^{(\mathrm{l})}\right\rangle_{t_1} = \hat{\mathrm{R}}^{(\mathrm{t,l})\rightarrow(\mathrm{l})}_{t_1}\left|\psi''^{(\mathrm{t,l})}\right\rangle = f\left(\xi_0\hat{a}^{\dagger}_{t_1,l_0} + \xi_1\hat{a}^{\dagger}_{t_1,l_1}\right)|0\rangle\,. \tag{70}$$

The success probability in this case is given by $\mathcal{S} = \left(\frac{1}{\sqrt{2}}\right)^2 = 0.5$. The discarded modes t_0 and t_2 in Eq.(69) do not carry any relevant information in interferometric setups, as only overlapping components of different paths can interfere with one another. Furthermore, one can eliminate the common mode t_1 and reformulate Eq.(70) as

$$\left|\psi^{(\mathrm{l})}\right\rangle = f\left(\xi_0\hat{a}^{\dagger}_{l_0} + \xi_1\hat{a}^{\dagger}_{l_1}\right)|0\rangle\,. \tag{71}$$

Comparing Eq.(71) with Eq.(65), it becomes evident that the time-bin information is effectively mapped to path line, indicating that a time-to-path mode mapping has occurred, as illustrated by

$$\begin{aligned}\left|\psi^{(\mathrm{l})}\right\rangle &= \hat{\mathrm{M}}^{(\mathrm{t})\rightarrow(\mathrm{l})}\left|\psi^{(\mathrm{t})}\right\rangle = \hat{\mathrm{R}}^{(\mathrm{t,l})\rightarrow(\mathrm{l})}_{t_1}\hat{\mathrm{T}}_{l_0}\left(\hat{\mathbb{1}}^{(\mathrm{t})}\otimes\hat{\mathrm{B}}^{(\mathrm{l})}\right)\hat{\mathrm{E}}^{(\mathrm{t})\rightarrow(\mathrm{t,l})}\left|\psi^{(\mathrm{t})}\right\rangle = f\left(\hat{a}^{\dagger(\mathrm{l})}_{\xi}\right)|0\rangle \\ &= f\left(\xi_0\hat{a}^{\dagger}_{l_0} + \xi_1\hat{a}^{\dagger}_{l_1}\right)|0\rangle\,,\end{aligned} \tag{72}$$

with fidelity $\mathcal{F} = 1$ and success probability $\mathcal{S} = 0.5$. This time-to-path mode mapping is widely implemented in the receiver for time-bin QKD that utilizes asymmetric Mach-Zehnder interferometer structures [24, 52].

4.3. Polarization-to-Path Mode Mapping

Consider a polarization-encoded quantum state represented as

$$\left|\psi^{(\mathrm{p})}\right\rangle = f\left(\hat{a}^{\dagger(\mathrm{p})}_{\xi}\right)|0\rangle = f\left(\xi_0\hat{a}^{\dagger}_{p_0} + \xi_1\hat{a}^{\dagger}_{p_1}\right)|0\rangle = f\left(\xi_0\hat{a}^{\dagger}_{h} + \xi_1\hat{a}^{\dagger}_{v}\right)|0\rangle\,, \tag{73}$$

where we assumed polarizations $p_0 = h$ and $p_1 = v$ denote the horizontal and vertical polarizations, respectively. Figure 7 illustrates a polarization-to-path mode mapping block, which includes a polarizing beam-splitter (PBS) followed by a half-waveplate (HWP), and an axillary polarizer (POL). Initially, the state $\left|\psi^{(\mathrm{p})}\right\rangle$ enters through port l_0 of the PBS, while the ground state $|0\rangle$ is introduced from port l_1, acting as a path mode expander

$$\left|\psi^{(\mathrm{p,l})}\right\rangle = \hat{\mathrm{E}}^{(\mathrm{p})\rightarrow(\mathrm{p,l})}\left|\psi^{(\mathrm{p})}\right\rangle = \left|\psi^{(\mathrm{p})}\right\rangle_{l_0}|0\rangle_{l_1} = f\left(\hat{a}^{\dagger(\mathrm{p,l})}_{\xi}\right)|0\rangle = f\left(\xi_0\hat{a}^{\dagger}_{h,l_0} + \xi_1\hat{a}^{\dagger}_{v,l_0}\right)|0\rangle\,. \tag{74}$$

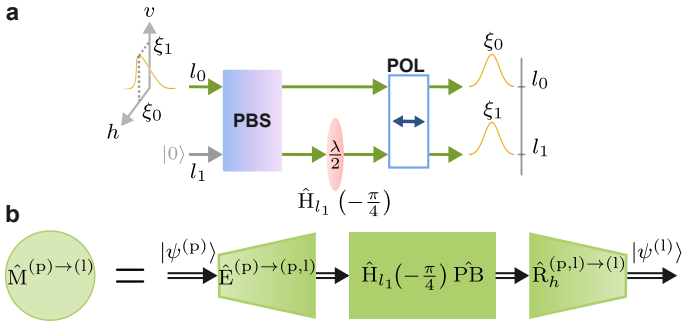

Fig. 7. Polarization-to-path mode mapper with $\mathcal{F} = 1$ and $\mathcal{S} = 1$. PBS: polarizing beam-splitter; $\frac{\lambda}{2}$: Half-waveplate; POL: polarizer.

Next, the PBS operator $\hat{\mathrm{PB}}$, which transmits horizontal polarization without altering its path line while reflecting vertical components by transferring their path line from l_0 to l_1, or vice versa, is applied within the (p,l) space as follows

$$\begin{aligned}\left|\psi'^{(\mathrm{p},\mathrm{l})}\right\rangle &= \hat{\mathrm{PB}}\left|\psi^{(\mathrm{p},\mathrm{l})}\right\rangle = \hat{\mathrm{PB}}\, f\left(\hat{a}^{\dagger(\mathrm{p},\mathrm{l})}_{\xi}\right)|0\rangle = \hat{\mathrm{PB}}\, f\left(\xi_0\hat{a}^{\dagger}_{h,l_0} + \xi_1\hat{a}^{\dagger}_{v,l_0}\right)|0\rangle \\ &= f\left(\xi_0\hat{a}^{\dagger}_{h,l_0} + \xi_1\hat{a}^{\dagger}_{v,l_1}\right)|0\rangle\,. \end{aligned} \tag{75}$$

Finally, the HWP on path l_1, set at an angle of $\theta = \frac{-\pi}{4}$, denoted as $\hat{\mathrm{H}}_{l_1}\left(-\frac{\pi}{4}\right)$, transforms $\hat{a}^{\dagger}_{v,l_1}$ into $\hat{a}^{\dagger}_{h,l_1}$. Consequently, we obtain

$$\left|\psi''^{(\mathrm{p},\mathrm{l})}\right\rangle = \hat{\mathrm{H}}_{l_1}\left(-\frac{\pi}{4}\right)\left|\psi'^{(\mathrm{p},\mathrm{l})}\right\rangle = f\left(\xi_0\hat{a}^{\dagger}_{h,l_0} + \xi_1\hat{a}^{\dagger}_{h,l_1}\right)|0\rangle\,. \tag{76}$$

Since Eq.(76) has no vertical components, the polarizer $\hat{\mathrm{P}}_h \equiv \hat{\mathrm{R}}_h^{(\mathrm{p},\mathrm{l})\to(\mathrm{l})}$, the mode reduction to the horizontal polarization, does not alter the quantum state of the signal, i.e., $\mathcal{S} = 1$. By disregarding the trivial polarization component h, Eq.(76) can be rewritten as

$$\left|\psi^{(\mathrm{l})}\right\rangle = \hat{\mathrm{R}}_h^{(\mathrm{p},\mathrm{l})\to(\mathrm{l})}\left|\psi''^{(\mathrm{p},\mathrm{l})}\right\rangle = f\left(\xi_0\hat{a}^{\dagger}_{l_0} + \xi_1\hat{a}^{\dagger}_{l_1}\right)|0\rangle = f\left(\hat{a}^{\dagger(\mathrm{l})}_{\xi}\right)|0\rangle\,. \tag{77}$$

Equations (73) and (77) yields

$$\begin{aligned}\left|\psi^{(\mathrm{l})}\right\rangle &= \hat{\mathrm{M}}^{(\mathrm{p})\to(\mathrm{l})}\left|\psi^{(\mathrm{p})}\right\rangle = \hat{\mathrm{M}}^{(\mathrm{p})\to(\mathrm{l})}\, f\left(\hat{a}^{\dagger(\mathrm{p})}_{\xi}\right)|0\rangle \\ &= \hat{\mathrm{R}}_h^{(\mathrm{p},\mathrm{l})\to(\mathrm{l})}\;\hat{\mathrm{H}}_{l_1}(-\frac{\pi}{4})\;\hat{\mathrm{PB}}\;\hat{\mathrm{E}}^{(\mathrm{p})\to(\mathrm{p},\mathrm{l})}\, f\left(\hat{a}^{\dagger(\mathrm{p})}_{\xi}\right)|0\rangle = f\left(\hat{a}^{\dagger(\mathrm{l})}_{\xi}\right)|0\rangle = f\left(\xi_0\hat{a}^{\dagger}_{l_0} + \xi_1\hat{a}^{\dagger}_{l_1}\right)|0\rangle\,, \end{aligned} \tag{78}$$

indicating a polarization-to-path mode mapping with fidelity $\mathcal{F} = 1$ and success probability $\mathcal{S} = 1$.

4.4. *Path-to-Polarization Mode Mapping*

Consider a path-encoded quantum signal as outlined in Eq.(59). Assume that the common polarization mode for components on paths l_0 and l_1 is horizontal polarization. This polarization mode is not indicated as a subscript of the creation operator since it does not convey any relevant information and remains invariant. A HWP set at an angle of $\theta = \frac{\pi}{4}$ on path l_1 transforms

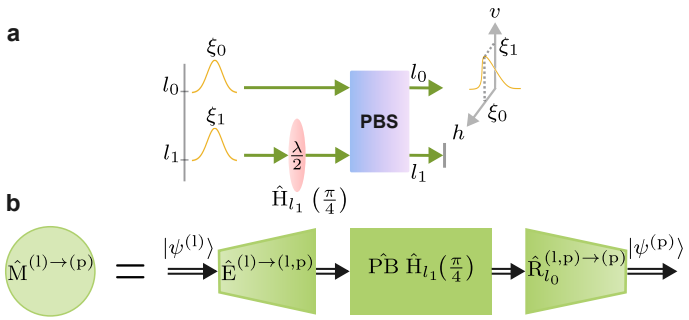

Fig. 8. Path-to-polarization mode mapper with $\mathcal{F} = 1$ and $\mathcal{S} = 1$. PBS: polarizing beam-splitter; $\frac{\lambda}{2}$: Half-waveplate.

$\hat{a}^\dagger_{l_1} \equiv \hat{a}^\dagger_{l_1,h}$ into $\hat{a}^\dagger_{l_1,v}$, as illustrated in Fig. 8. In this scenario, applying the HWP requires a mode expander to include the polarization, leading to the following expression

$$\left|\psi^{(\mathrm{l,p})}\right\rangle = \hat{\mathrm{E}}^{(\mathrm{l})\to(\mathrm{l,p})}\left|\psi^{(\mathrm{l})}\right\rangle = f\left(\hat{a}^{\dagger(\mathrm{l,p})}_{\xi}\right)|0\rangle = f\left(\xi_0\hat{a}^\dagger_{l_0,h} + \xi_1\hat{a}^\dagger_{l_1,h}\right)|0\rangle\,. \tag{79}$$

Subsequently, utilizing the HWP operator on path l_1, configured at an angle of $\theta = \frac{\pi}{4}$ and represented as $\hat{\mathrm{H}}_{l_1}\left(\frac{\pi}{4}\right)$, results in

$$\left|\psi'^{(\mathrm{l,p})}\right\rangle = \hat{\mathrm{H}}_{l_1}\left(\frac{\pi}{4}\right)\left|\psi^{(\mathrm{l,p})}\right\rangle = f\left(\xi_0\hat{a}^\dagger_{l_0,h} + \xi_1\hat{a}^\dagger_{l_1,v}\right)|0\rangle\,. \tag{80}$$

Following this, the PBS operator $\hat{\mathrm{PB}}$ transforms $\hat{a}^\dagger_{l_1,v}$ into $\hat{a}^\dagger_{l_0,v}$, resulting in

$$\left|\psi''^{(\mathrm{l,p})}\right\rangle = \hat{\mathrm{PB}}\left|\psi'^{(\mathrm{l,p})}\right\rangle = f\left(\xi_0\hat{a}^\dagger_{l_0,h} + \xi_1\hat{a}^\dagger_{l_0,v}\right)|0\rangle\,. \tag{81}$$

By blocking the path line l_1, which is associated with the mode reduction operator $\hat{\mathrm{R}}_{l_0}^{(\mathrm{l,p})\to(\mathrm{p})}$ with $\mathcal{S} = 1$, one arrives at the polarization-encoded state

$$\begin{aligned}\left|\psi^{(\mathrm{p})}\right\rangle &= \hat{\mathrm{M}}^{(\mathrm{l})\to(\mathrm{p})}\left|\psi^{(\mathrm{l})}\right\rangle = \hat{\mathrm{M}}^{(\mathrm{l})\to(\mathrm{p})} f\left(\hat{a}^{\dagger(\mathrm{l})}_{\xi}\right)|0\rangle \\ &= \hat{\mathrm{R}}_{l_0}^{(\mathrm{l,p})\to(\mathrm{p})}\ \hat{\mathrm{PB}}\ \hat{\mathrm{H}}_{l_1}\left(\frac{\pi}{4}\right)\ \hat{\mathrm{E}}^{(\mathrm{l})\to(\mathrm{l,p})} f\left(\hat{a}^{\dagger(\mathrm{l})}_{\xi}\right)|0\rangle = f\left(\hat{a}^{\dagger(\mathrm{p})}_{\xi}\right)|0\rangle = f\left(\xi_0\hat{a}^\dagger_h + \xi_1\hat{a}^\dagger_v\right)|0\rangle\,.\end{aligned} \tag{82}$$

This represents a mapping from path to polarization mode with fidelity $\mathcal{F} = 1$ and success probability $\mathcal{S} = 1$.

4.5. Polarization-to-Time Mode Mapping via Birefringent Crystal

Consider a polarization-encoded quantum state as outlined in Eq.(73). To implement a polarization-to-time mode mapper, one can utilize a combination of a polarization-to-path mode mapper (Fig. 7) followed by a path-to-time mode mapper (Fig. 5). This configuration effectively transforms the polarization carriers of quantum information into temporal carriers, with $\mathcal{S} = 1\times0.5 \equiv 0\text{dB} - 3\text{dB}$. However, in this subsection, we aim to present an alternative polarization-to-time mode mapper characterized by time separation on the order of picoseconds. This mapper is employed in the transmitter of the ultrafast time-bin qubits [14] and qudits [53].

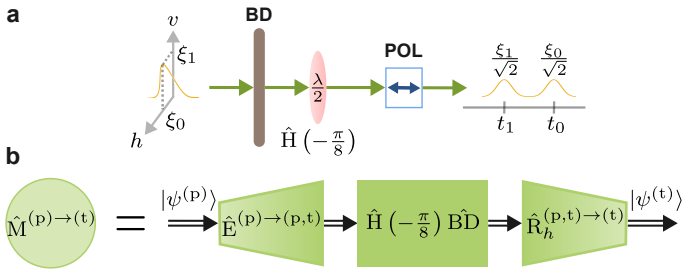

Fig. 9. Polarization-to-time mode mapper via birefringent crystal, with $\mathcal{F} = 1$ and $\mathcal{S} = 0.5$. $\frac{\lambda}{2}$: Half-waveplate; POL: polarizer; BD: birefringent time delay crystal.

As depicted in Fig. 9, a birefringent time delay crystal (such as the α-BBO crystal) is utilized in this structure, which introduces different delays to the orthogonal polarization components described in Eq.(73), specifically

$$\left|\psi'^{(\mathrm{p,t})}\right\rangle = \hat{\mathrm{BD}}\,\hat{\mathrm{E}}^{(\mathrm{p})\to(\mathrm{p,t})}\left|\psi^{(\mathrm{p})}\right\rangle = f\left(\xi_0\hat{a}^{\dagger}_{h,t_0} + \xi_1\hat{a}^{\dagger}_{v,t_1}\right)|0\rangle\,, \tag{83}$$

where $\hat{\mathrm{BD}}$ represents the birefringent time delay operator. Following that, a HWP configured at an angle of $-\frac{\pi}{8}$ is applied to the state described in Eq.(83), leading to

$$\left|\psi''^{(\mathrm{p,t})}\right\rangle = \hat{\mathrm{H}}\left(-\frac{\pi}{8}\right)\left|\psi'^{(\mathrm{p,t})}\right\rangle = f\left(\hat{a}^{\dagger(\mathrm{p,t})}_{\xi''}\right)|0\rangle\,, \tag{84}$$

where

$$\hat{a}^{\dagger(\mathrm{p,t})}_{\xi''} = \xi_0\hat{a}^{\dagger}_{a,t_0} + \xi_1\hat{a}^{\dagger}_{d,t_1} = \frac{\xi_0\hat{a}^{\dagger}_{h,t_0} - \xi_0\hat{a}^{\dagger}_{v,t_0} + \xi_1\hat{a}^{\dagger}_{h,t_1} + \xi_1\hat{a}^{\dagger}_{v,t_1}}{\sqrt{2}}. \tag{85}$$

The subscripts d and a in Eq.(85) represent diagonal and anti-diagonal polarizations, corresponding to angles of $\frac{\pi}{4}$ and $-\frac{\pi}{4}$, respectively. Subsequently, the state $\left|\psi''^{(\mathrm{p,t})}\right\rangle$ passes through a polarizer that transmits horizontal polarization, $\hat{\mathrm{P}}_h \equiv \hat{\mathrm{R}}_h^{(\mathrm{p,t})\to(\mathrm{t})}$, results in the time-encoded quantum state as follows

$$\left|\psi^{(\mathrm{t})}\right\rangle = \hat{\mathrm{P}}_h\left|\psi''^{(\mathrm{p,t})}\right\rangle = \hat{\mathrm{R}}_h^{(\mathrm{p,t})\to(\mathrm{t})}\left|\psi''^{(\mathrm{p,t})}\right\rangle = f\left(\xi_0\hat{a}^{\dagger}_{h,t_0} + \xi_1\hat{a}^{\dagger}_{h,t_1}\right)|0\rangle \equiv f\left(\xi_0\hat{a}^{\dagger}_{t_0} + \xi_1\hat{a}^{\dagger}_{t_1}\right)|0\rangle\,. \tag{86}$$

with fidelity $\mathcal{F} = 1$ and success probability $\mathcal{S} = 0.5$. A comparison between Eq.(73) and Eq.(86) reveals a polarization-to-time mode mapping operation characterized by fidelity $\mathcal{F} = 1$ and success probability $\mathcal{S} = 0.5$. Specifically, we have

$$\begin{aligned}\left|\psi^{(\mathrm{t})}\right\rangle &= \hat{\mathrm{M}}^{(\mathrm{p})\to(\mathrm{t})}\left|\psi^{(\mathrm{p})}\right\rangle = \hat{\mathrm{R}}_h^{(\mathrm{p,t})\to(\mathrm{t})}\hat{\mathrm{H}}\left(-\frac{\pi}{8}\right)\hat{\mathrm{BD}}\,\hat{\mathrm{E}}^{(\mathrm{p})\to(\mathrm{p,t})} f\left(\hat{a}^{\dagger(\mathrm{p})}_{\xi}\right)|0\rangle = f\left(\hat{a}^{\dagger(\mathrm{t})}_{\xi}\right)|0\rangle \\ &= f\left(\xi_0\hat{a}^{\dagger}_{t_0} + \xi_1\hat{a}^{\dagger}_{t_1}\right)|0\rangle\,.\end{aligned} \tag{87}$$

4.6. Time-to-Polarization Mode Mapping

Consider a time-encoded quantum state as described in Eq.(65). To implement a time-to-polarization mode mapper, one can utilize a sequential approach involving a time-to-path mode mapper (illustrated in Fig. 6), followed by a path-to-polarization mode mapper (shown in Fig. 8).

This configuration effectively transforms the temporal carriers of quantum information into polarization carriers, with success probability $\mathcal{S} = 0.5$. However, in this subsection, we aim to introduce another time-to-polarization mode mapper that accurately converts the picosecond-separated time bins discussed in subsection 4.5 back into polarization states. The efficacy of this structure has been experimentally demonstrated in [54] and subsequently applied in the reception of ultrafast time-bin qubits [14] and qudits [53].

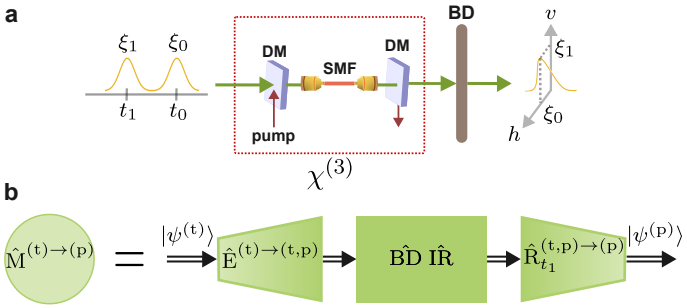

Fig. 10. Time-to-polarization mode mapper with $\mathcal{F} = 1$ and $\mathcal{S} = 1$. DM: dichroic mirror; SMF: sinlge mode fiber; BD: birefringent time delay crystal.

Consider the quantum information is encoded in the temporal degree of a quantum signal, as described in Eq.(65). Figure 10 depicts the time-to-polarization mode mapping setup. A synchronized pump pulse at time t_1, characterized by a specific wavelength and polarization, is combined with the signal pulse using a dichroic mirror (DM) and subsequently coupled into a single-mode fiber (SMF). The strong pump pulse in the SMF creates a third-order nonlinearity that induces birefringence. This birefringence rotates the polarization of the components of the signal pulse at time t_1 through cross-phase modulation, which occurs due to the optical Kerr effect [54]. Consequently,

$$\left|\psi'^{(t,p)}\right\rangle = \hat{IR}\ \hat{E}^{(t)\to(t,p)} \left|\psi^{(t)}\right\rangle = f\left(\hat{a}^{\dagger(t,p)}_{\xi'}\right)|0\rangle = f\left(\xi_0 \hat{a}^{\dagger}_{t_0,h} + \xi_1 \hat{a}^{\dagger}_{t_1,v}\right)|0\rangle\,. \tag{88}$$

where $\hat{IR}$ represents the induced rotation operation of the SMF. In the next step, a birefringent time delay crystal, which has the same thickness as that described in subsection 4.5, introduces a greater delay for the horizontal component compared to the vertical component. This can be expressed mathematically as follows

$$\left|\psi''^{(t,p)}\right\rangle = \hat{BD} \left|\psi'^{(t,p)}\right\rangle = f\left(\hat{a}^{\dagger(t,p)}_{\xi''}\right)|0\rangle = f\left(\xi_0 \hat{a}^{\dagger}_{t_1,h} + \xi_1 \hat{a}^{\dagger}_{t_1,v}\right)|0\rangle\,, \tag{89}$$

where $\hat{BD}$ represents the corresponding quantum operator for the birefringent time delay crystal. Since the quantum signal has only temporal component t_1, the mode reduction to this time slot, i.e., $\hat{R}_{t_1}^{(t,p)\to(p)}$, is equivalent to the identity operator for the quantum signal of Eq.(89). Therefore, by discarding the trivial temporal mode t_1, we arrive at

$$\left|\psi^{(p)}\right\rangle = f\left(\hat{a}^{\dagger(p)}_{\xi}\right)|0\rangle = f\left(\xi_0 \hat{a}^{\dagger}_{h} + \xi_1 \hat{a}^{\dagger}_{v}\right)|0\rangle\,. \tag{90}$$

A comparison of Eq.(65) with Eq.(90) reveals a time-to-polarization mode mapping operation, which can be expressed as

$$\begin{aligned}\left|\psi^{(p)}\right\rangle &= \hat{M}^{(t)\to(p)} \left|\psi^{(t)}\right\rangle = \hat{R}_{t_1}^{(t,p)\to(p)}\ \hat{BD}\ \hat{IR}\ \hat{E}^{(t)\to(t,p)} \left|\psi^{(t)}\right\rangle = f\left(\hat{a}^{\dagger(p)}_{\xi}\right)|0\rangle \\ &= f\left(\xi_0 \hat{a}^{\dagger}_{h} + \xi_1 \hat{a}^{\dagger}_{v}\right)|0\rangle\,.\end{aligned} \tag{91}$$

This mapping operation is characterized by fidelity $\mathcal{F} = 1$ and success probability $\mathcal{S} = 1$.

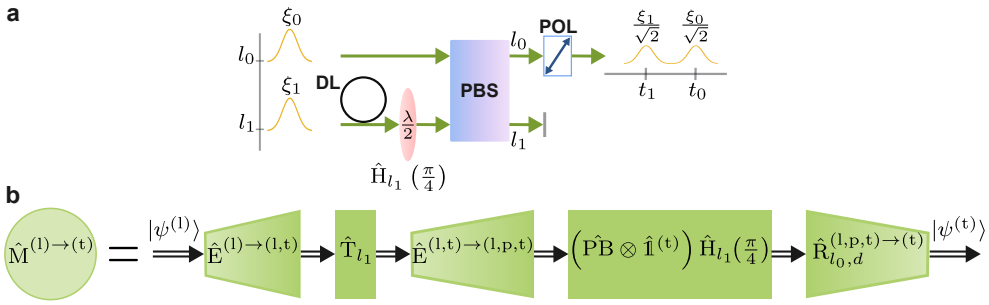

Fig. 11. Path-to-time mode mapper via polarizing beam-splitter with $\mathcal{F} = 1$ and $\mathcal{S} = 0.5$. DL: delay line; $\frac{\lambda}{2}$: Half-waveplate; PBS: polarizing beam-splitter; POL: polarizer.

Consider a path-encoded quantum state as described in Eq.(59). In subsection 4.1, a path-to-time mode mapping module is introduced, utilizing a delay line and a beam-splitter. Figure 11 illustrates an alternative path-to-time mode mapper employing a PBS. The effect of the time delay on line l_1, $\hat{T}_{l_1}$, on the path-encoded state is described as follows

$$\left|\psi^{(l,t)}\right\rangle = \hat{T}_{l_1}\ \hat{E}^{(l)\to(l,t)}\left|\psi^{(l)}\right\rangle = f\left(\xi_0\hat{a}^{\dagger}_{l_0,t_0} + \xi_1\hat{a}^{\dagger}_{l_1,t_1}\right)|0\rangle\,. \tag{92}$$

The two creation operators $\hat{a}^{\dagger}_{l_0,t_0}$ and $\hat{a}^{\dagger}_{l_1,t_1}$ share a common polarization mode, for instance, horizontal polarization. This horizontal polarization is not explicitly included as a subscript in the creation operator, as it does not provide additional information and remains constant. However, when a half-wave plate with an angle of $\theta = \frac{\pi}{4}$ is applied to path line l_1,the horizontal component is transformed into vertical polarization. Thus, the state can be represented as follows

$$\left|\psi'^{(l,p,t)}\right\rangle = \hat{H}_{l_1}(\frac{\pi}{4})\ \hat{E}^{(l,t)\to(l,p,t)}\left|\psi^{(l,t)}\right\rangle = f\left(\xi_0\hat{a}^{\dagger}_{l_0,h,t_0} + \xi_1\hat{a}^{\dagger}_{l_1,v,t_1}\right). \tag{93}$$

The polarizing beam-splitter operator $\hat{PB}$ switches the path mode when the input polarization is vertical. Moreover, $\hat{PB}$ does not influence the temporal components. Consequently, the output quantum state of the PBS can be expressed as follows

$$\left|\psi''^{(l,p,t)}\right\rangle = \left(P\hat{B}\otimes\hat{1}^{(t)}\right)\left|\psi'^{(l,p,t)}\right\rangle = f\left(\xi_0\hat{a}^{\dagger}_{l_0,h,t_0} + \xi_1\hat{a}^{\dagger}_{l_0,v,t_1}\right)|0\rangle\,. \tag{94}$$

Mode reduction to path l_0 and discarding the common path l_0 from notation gives

$$\left|\psi''^{(p,t)}\right\rangle = \hat{R}^{(l,p,t)\to(p,t)}_{l_0}\left|\psi''^{(l,p,t)}\right\rangle = f\left(\xi_0\hat{a}^{\dagger}_{h,t_0} + \xi_1\hat{a}^{\dagger}_{v,t_1}\right)|0\rangle = f\left(\hat{a}^{\dagger(p,t)}_{\xi}\right)|0\rangle\,. \tag{95}$$

This path reduction happens with to success probability $\mathcal{S} = 1$. To complete the path-to-time mode mapping, it is essential that all components of Eq.(95) have identical polarization. However, one can extract the quantum information without concern for the polarization components via an appropriate measurement scheme [55].

To erase polarization information, a polarizer that transmits diagonal polarization can be employed. Rewriting Eq.(95) in terms of diagonal and anti-diagonal polarization results in the following expression

$$\hat{a}^{\dagger(p,t)}_{\xi} = \frac{\xi_0}{\sqrt{2}}\hat{a}^{\dagger}_{d,t_0} + \frac{\xi_0}{\sqrt{2}}\hat{a}^{\dagger}_{a,t_0} + \frac{\xi_1}{\sqrt{2}}\hat{a}^{\dagger}_{d,t_1} - \frac{\xi_1}{\sqrt{2}}\hat{a}^{\dagger}_{a,t_1}. \tag{96}$$

In this case, the polarizer exclusively transmits the diagonal components while blocking the others, leading to the following reduced state

$$\left|\psi^{(\mathrm{t})}\right\rangle = \hat{\mathrm{R}}_{d}^{(\mathrm{p,t})\to(\mathrm{t})} \left|\psi''^{(\mathrm{p,t})}\right\rangle = f\left(\xi_0 \hat{a}^{\dagger}_{d,t_0} + \xi_1 \hat{a}^{\dagger}_{d,t_1}\right)|0\rangle = f\left(\xi_0 \hat{a}^{\dagger}_{t_0} + \xi_1 \hat{a}^{\dagger}_{t_1}\right)|0\rangle\,. \tag{97}$$

with success probability $\mathcal{S} = 0.5$. It's worth noting that the rotational angle 45° of the polarizer has been chosen such that the ratio of the two temporal components remains unchanged after normalization. By comparing Eq.(97) with Eq.(59), we can identify a path-to-time mode mapping operation, specifically

$$\begin{aligned}\left|\psi^{(\mathrm{t})}\right\rangle &= \hat{\mathrm{M}}^{(\mathrm{l})\to(\mathrm{t})} \left|\psi^{(\mathrm{l})}\right\rangle = \hat{\mathrm{R}}_{d,l_0}^{(\mathrm{l,p,t})\to(\mathrm{t})} \left(\hat{\mathrm{PB}} \otimes \hat{\mathbb{1}}^{(\mathrm{t})}\right) \hat{\mathrm{H}}_{l_1}(\tfrac{\pi}{4})\, \hat{\mathrm{E}}^{(\mathrm{l,t})\to(\mathrm{l,p,t})}\, \hat{\mathrm{T}}_{l_1}\, \hat{\mathrm{E}}^{(\mathrm{l})\to(\mathrm{l,t})} f\left(\hat{a}^{\dagger(\mathrm{l})}_{\xi}\right)|0\rangle \\ &= f\left(\xi_0 \hat{a}^{\dagger}_{t_0} + \xi_1 \hat{a}^{\dagger}_{t_1}\right)|0\rangle\,,\end{aligned} \tag{98}$$

with $\mathcal{F} = 1$ and $\mathcal{S} = 0.5$, where

$$\hat{\mathrm{R}}_{l_0,d}^{(\mathrm{l,p,t})\to(\mathrm{t})} = \hat{\mathrm{R}}_{d}^{(\mathrm{p,t})\to(\mathrm{t})}\, \hat{\mathrm{R}}_{l_0}^{(\mathrm{l,p,t})\to(\mathrm{p,t})}\,. \tag{99}$$

This path-to-time mode mapping is employed in the transmitter of practical interferometric QKD protocols [12, 56, 57], as well as in QKD metropolitan networks [58].

4.8. *Polarization-to-Time Mode Mapping via Delay Line*

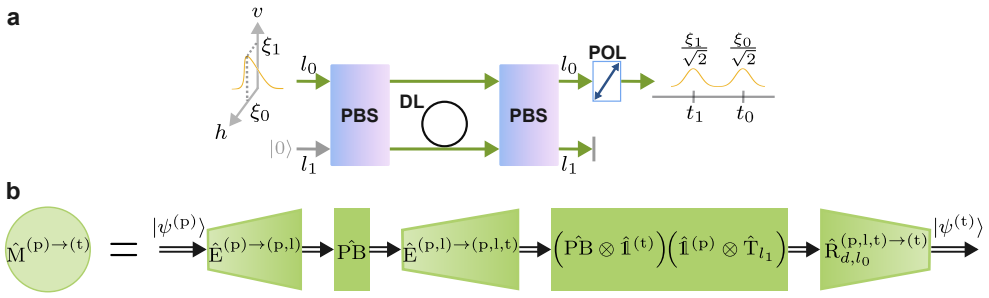

Fig. 12. Polarization-to-time mode mapper via delay line with $\mathcal{F} = 1$ and $\mathcal{S} = 0.5$. DL: delay line; PBS: polarizing beam-splitter; POL: polarizer.

While Fig. 9 illustrates a polarization-to-time mode mapping, the separation time between time bins is dictated by the thickness of the birefringent time delay crystal, which is on the order of a few millimeters, resulting in a separation time of picoseconds. This duration may be inadequate, particularly in detectors with approximately 1 nanosecond timing jitter. Figure 12 presents an alternative polarization-to-time mode mapper, which consists of the polarization-to-path mode mapper shown in Fig. 7, followed by the path-to-polarization mode mapper depicted in Fig. 11. It is important to note that the two half-wave plates effectively cancel each other's influence due to their opposing angles of $\frac{\pi}{4}$ and $-\frac{\pi}{4}$. Therefore, also the auxiliary polarizer in Fig. 7 is removed. Consequently, we have

$$\begin{aligned}\left|\psi^{(\mathrm{t})}\right\rangle &= \hat{\mathrm{M}}^{(\mathrm{p})\to(\mathrm{t})} \left|\phi^{(\mathrm{p})}\right\rangle = \hat{\mathrm{M}}^{(\mathrm{l})\to(\mathrm{t})} \hat{\mathrm{M}}^{(\mathrm{p})\to(\mathrm{l})} f\left(\xi_0 \hat{a}^{\dagger}_{p_0} + \xi_1 \hat{a}^{\dagger}_{p_1}\right)|0\rangle \\ &= \hat{\mathrm{R}}_{d,l_0}^{(\mathrm{p,l,t})\to(\mathrm{t})} \left(\hat{\mathrm{PB}} \otimes \hat{\mathbb{1}}^{(\mathrm{t})}\right) \left(\hat{\mathbb{1}}^{(\mathrm{p})} \otimes \hat{\mathrm{T}}_{l_1}\right) \hat{\mathrm{E}}^{(\mathrm{p,l})\to(\mathrm{p,l,t})}\, \hat{\mathrm{PB}}\, \hat{\mathrm{E}}^{(\mathrm{p})\to(\mathrm{p,l})} f\left(\xi_0 \hat{a}^{\dagger}_{p_0} + \xi_1 \hat{a}^{\dagger}_{p_1}\right)|0\rangle \\ &= f\left(\xi_0 \hat{a}^{\dagger}_{t_0} + \xi_1 \hat{a}^{\dagger}_{t_1}\right)|0\rangle\,.\end{aligned} \tag{100}$$

Here, we consider the path to time mode mapping of subsection 4.7 with utilizing a polarizer, which has $\mathcal{S} = 0.5$. Therefore, the success probability of the scheme of Fig. 12 is $\mathcal{S} = 1{\times}0.5 = 0.5$, where this value is the product of success probability of two aforementioned structures. This polarization-to-time mode mapper is also employed in the receiver of the ultrafast time-bin QKD structure [14, 53].

5. Conclusion

In this paper, we explored the fundamental mathematical frameworks essential for mode adaptation in quantum communication processors. Through an in-depth analysis of the mathematical frameworks governing mode expansion, reduction, and mapping, we highlighted their critical roles in enhancing the interoperability among various operators within a quantum processor and different quantum nodes in a network. Table 1 summarizes mode mapping schemes studied in this paper, highlighting their quantum operators, fidelity, and success probability. These frameworks not only provide a deeper understanding of optical quantum signal manipulation but also establish a foundation for practical applications that can drive the advancement of the Quantum Internet.

Furthermore, the interplay between different optical implementations emphasizes the significance of mode adaptability, particularly in addressing real-world challenges in quantum communication. The insights gained from our research could lead to more resilient and versatile quantum communication frameworks, ultimately enhancing the prospects for robust quantum data exchange in an increasingly interconnected quantum network.

Table 1. Summary of Various mode mapping schemes.

MM.	Subsec.	Quantum operator	$\mathcal{F}$	$\mathcal{S}$
$\hat{\mathrm{M}}^{(\mathrm{l})\to(\mathrm{t})}$	4.1	$\hat{\mathrm{R}}_{l_0}^{(\mathrm{l,t})\to(\mathrm{t})}\left(\hat{\mathrm{B}}^{(\mathrm{l})}\otimes\hat{\mathbb{1}}^{(\mathrm{t})}\right)\hat{\mathrm{T}}_{l_1}\hat{\mathrm{E}}^{(\mathrm{l})\to(\mathrm{l,t})}$	1	0.5
$\hat{\mathrm{M}}^{(\mathrm{t})\to(\mathrm{l})}$	4.2	$\hat{\mathrm{R}}_{t_1}^{(\mathrm{t,l})\to(\mathrm{l})}\hat{\mathrm{T}}_{l_0}\left(\hat{\mathbb{1}}^{(\mathrm{t})}\otimes\hat{\mathrm{B}}^{(\mathrm{l})}\right)\hat{\mathrm{E}}^{(\mathrm{t})\to(\mathrm{t,l})}$	1	0.5
$\hat{\mathrm{M}}^{(\mathrm{p})\to(\mathrm{l})}$	4.3	$\hat{\mathrm{R}}_{h}^{(\mathrm{p,l})\to(\mathrm{l})}\ \hat{\mathrm{H}}_{l_1}(-\frac{\pi}{4})\ \hat{\mathrm{PB}}\ \hat{\mathrm{E}}^{(\mathrm{p})\to(\mathrm{p,l})}$	1	1
$\hat{\mathrm{M}}^{(\mathrm{l})\to(\mathrm{p})}$	4.4	$\hat{\mathrm{R}}_{l_0}^{(\mathrm{l,p})\to(\mathrm{p})}\ \hat{\mathrm{PB}}\ \hat{\mathrm{H}}_{l_1}\left(\frac{\pi}{4}\right)\ \hat{\mathrm{E}}^{(\mathrm{l})\to(\mathrm{l,p})}$	1	1
$\hat{\mathrm{M}}^{(\mathrm{p})\to(\mathrm{t})}$	4.5	$\hat{\mathrm{R}}_{h}^{(\mathrm{p,t})\to(\mathrm{t})}\hat{\mathrm{H}}\left(-\frac{\pi}{8}\right)\ \hat{\mathrm{BD}}\ \hat{\mathrm{E}}^{(\mathrm{p})\to(\mathrm{p,t})}$	1	0.5
$\hat{\mathrm{M}}^{(\mathrm{t})\to(\mathrm{p})}$	4.6	$\hat{\mathrm{R}}_{t_1}^{(\mathrm{t,p})\to(\mathrm{p})}\ \hat{\mathrm{BD}}\ \hat{\mathrm{IR}}\ \hat{\mathrm{E}}^{(\mathrm{t})\to(\mathrm{t,p})}$	1	1
$\hat{\mathrm{M}}^{(\mathrm{l})\to(\mathrm{t})}$	4.7	$\hat{\mathrm{R}}_{l_0,d}^{(\mathrm{l,p,t})\to(\mathrm{t})}\left(\hat{\mathrm{PB}}\otimes\hat{\mathbb{1}}^{(\mathrm{t})}\right)\hat{\mathrm{H}}_{l_1}(\frac{\pi}{4})\ \hat{\mathrm{E}}^{(\mathrm{l,t})\to(\mathrm{l,p,t})}\ \hat{\mathrm{T}}_{l_1}\ \hat{\mathrm{E}}^{(\mathrm{l})\to(\mathrm{l,t})}$	1	0.5
$\hat{\mathrm{M}}^{(\mathrm{p})\to(\mathrm{t})}$	4.8	$\hat{\mathrm{R}}_{d,l_0}^{(\mathrm{p,l,t})\to(\mathrm{t})}\left(\hat{\mathrm{PB}}\otimes\hat{\mathbb{1}}^{(\mathrm{t})}\right)\left(\hat{\mathbb{1}}^{(\mathrm{p})}\otimes\hat{\mathrm{T}}_{l_1}\right)\hat{\mathrm{E}}^{(\mathrm{p,l})\to(\mathrm{p,l,t})}\ \hat{\mathrm{PB}}\ \hat{\mathrm{E}}^{(\mathrm{p})\to(\mathrm{p,l})}$	1	0.5

A. Evolution of the Photon Creation Operator

Let us investigate the effect of an arbitrary unitary operator $\hat{\mathrm{U}}^{(\mathrm{m})}$ on a quantum state described by a creation operator $\hat{a}_{\xi}^{\dagger(\mathrm{m})}$, i.e.,

$$\left|\psi^{(\mathrm{m})}\right\rangle = f\left(\hat{a}_{\xi}^{\dagger(\mathrm{m})}\right)|0\rangle\,. \tag{A.1}$$

Since the $f\left(\hat{a}_{\xi}^{\dagger(\mathrm{m})}\right)$ function is analytic and arbitrary differentiable, it can be expanded using its Taylor series as follows

$$f\left(\hat{a}_{\xi}^{\dagger(\mathrm{m})}\right) = f(0) + f'(0)\hat{a}_{\xi}^{\dagger(\mathrm{m})} + \frac{f''(0)}{2!}\left(\hat{a}_{\xi}^{\dagger(\mathrm{m})}\right)^2 + \frac{f'''(0)}{3!}\left(\hat{a}_{\xi}^{\dagger(\mathrm{m})}\right)^3 + \ldots \tag{A.2}$$

Furthermore, due to the unitarity of the operator $\hat{\mathrm{U}}^{(\mathrm{m})}$, which satisfies the relation $\hat{\mathrm{U}}^{\dagger(\mathrm{m})}\hat{\mathrm{U}}^{(\mathrm{m})} = \hat{\mathbb{1}}$, one can write

$$\begin{aligned}\hat{\mathrm{U}}^{(\mathrm{m})}(\hat{a}_{\xi}^{\dagger(\mathrm{m})})^n\hat{\mathrm{U}}^{\dagger(\mathrm{m})} &= \hat{\mathrm{U}}^{(\mathrm{m})}\hat{a}_{\xi}^{\dagger(\mathrm{m})}\hat{\mathrm{U}}^{\dagger(\mathrm{m})}\hat{\mathrm{U}}^{(\mathrm{m})}\hat{a}_{\xi}^{\dagger(\mathrm{m})}\hat{\mathrm{U}}^{\dagger(\mathrm{m})}\ldots\hat{\mathrm{U}}^{(\mathrm{m})}\hat{a}_{\xi}^{\dagger(\mathrm{m})}\hat{\mathrm{U}}^{\dagger(\mathrm{m})} \\ &= \left(\hat{\mathrm{U}}^{(\mathrm{m})}\hat{a}_{\xi}^{\dagger(\mathrm{m})}\hat{\mathrm{U}}^{\dagger(\mathrm{m})}\right)^n.\end{aligned} \tag{A.3}$$

Using Eq.(A.2) and Eq.(A.3), it can simply be concluded that

$$\hat{\mathrm{U}}^{(\mathrm{m})} f\left(\hat{a}_{\xi}^{\dagger(\mathrm{m})}\right)\hat{\mathrm{U}}^{\dagger(\mathrm{m})} = f\left(\hat{\mathrm{U}}^{(\mathrm{m})}\hat{a}_{\xi}^{\dagger(\mathrm{m})}\hat{\mathrm{U}}^{\dagger(\mathrm{m})}\right). \tag{A.4}$$

Therefore, applying the unitary operator $\hat{\mathrm{U}}^{(\mathrm{m})}$ on the quantum state $\left|\psi^{(\mathrm{m})}\right\rangle$ is expandable as [47]

$$\begin{aligned}\left|\psi'^{(\mathrm{m})}\right\rangle = \hat{\mathrm{U}}^{(\mathrm{m})}\left|\psi^{(\mathrm{m})}\right\rangle &= \hat{\mathrm{U}}^{(\mathrm{m})} f\left(\hat{a}_{\xi}^{\dagger(\mathrm{m})}\right)|0\rangle = \hat{\mathrm{U}}^{(\mathrm{m})} f\left(\hat{a}_{\xi}^{\dagger(\mathrm{m})}\right)\hat{\mathrm{U}}^{\dagger(\mathrm{m})}|0\rangle \\ &= f\left(\hat{\mathrm{U}}^{(\mathrm{m})}\hat{a}_{\xi}^{\dagger(\mathrm{m})}\hat{\mathrm{U}}^{\dagger(\mathrm{m})}\right)|0\rangle = f\left(\hat{a}_{\xi'}^{\dagger(\mathrm{m})}\right)|0\rangle,\end{aligned} \tag{A.5}$$

where $\hat{a}_{\xi'}^{\dagger(\mathrm{m})} = \hat{\mathrm{U}}^{(\mathrm{m})}\hat{a}_{\xi}^{\dagger(\mathrm{m})}\hat{\mathrm{U}}^{\dagger(\mathrm{m})}$, and the unitary of $\hat{\mathrm{U}}^{(\mathrm{m})}$, which ensures that $\hat{\mathrm{U}}^{\dagger(\mathrm{m})}|0\rangle = |0\rangle$, is utilized.

Consider the creation operator $\hat{a}_{\xi}^{\dagger(\mathrm{m})}$ is defined in the d-dimensional signal space associated with signal mode (m). Therefore, the input photon creation operator, indicated in Eq.(A.1), can be expressed as

$$\hat{a}_{\xi}^{\dagger(\mathrm{m})} = \sum_{i=0}^{d-1}\xi_i\hat{a}_{m_i}^{\dagger}. \tag{A.6}$$

It can be shown that, for lossless linear optical devices, the field operators transform as [47, 59–61]

$$\hat{\mathrm{U}}^{(\mathrm{m})}\hat{a}_{m_j}^{\dagger}\hat{\mathrm{U}}^{\dagger(\mathrm{m})} = \sum_{i=0}^{d-1}u_{i,j}\;\hat{a}_{m_i}^{\dagger}, \tag{A.7}$$

where the field transformation matrix $\mathbf{U}$ with elements $u_{i,j}$ is a d-dimensional unitary matrix associated with the unitary operator $\hat{\mathrm{U}}$ in the Fock space. Consequently, one can derive the following expression

$$\hat{a}_{\xi'}^{\dagger(\mathrm{m})} = \sum_{j=0}^{d-1}\xi_j\hat{\mathrm{U}}^{(\mathrm{m})}\hat{a}_{m_j}^{\dagger}\hat{\mathrm{U}}^{\dagger(\mathrm{m})} = \sum_{j=0}^{d-1}\xi_j\left(\sum_{i=0}^{d-1}u_{i,j}\;\hat{a}_{m_i}^{\dagger}\right) = \sum_{i=0}^{d-1}\xi_i'\;\hat{a}_{m_i}^{\dagger}, \tag{A.8}$$

where

$$\xi_i' = \sum_{j=0}^{d-1}u_{i,j}\;\xi_j, \tag{A.9}$$

which is identical to its counterpart in quantum information processing, as shown in Eq.(9).

B. Towards Mode Expansion Coefficients

Consider applying a mode expansion operator, denoted by $\hat{\mathrm{E}}$, to an arbitrary quantum state $\left|\psi\right\rangle \in \mathcal{H}_d$, as outlined in Eq.(1). The evolution of an informational quantum state is described in Eq.(8) through the application of a unitary operator. In a similar manner, the expanded quantum state $\left|\psi_{\mathrm{E}}\right\rangle \in \mathcal{H}_{d_{\mathrm{e}}}$ can be expressed in terms of logical bases represented by $|k\rangle_L$, where $0 \leq k < d_{\mathrm{e}}$. This leads to the following expression

$$\left|\psi_{\mathrm{E}}\right\rangle = \hat{\mathrm{E}}\left|\psi\right\rangle = \hat{\mathrm{E}} \sum_{i=0}^{d-1} \xi_i \, |i\rangle_L = \sum_{k=0}^{d_{\mathrm{e}}-1} \xi'_k \, |k\rangle_L \,, \tag{B.1}$$

where ξ'_k signifies the probability amplitude associated with the k-th logical basis $|k\rangle_L$. Since Eq.(B.1) represents the expanded quantum state within the expanded Hilbert space $\mathcal{H}_{d_{\mathrm{e}}}$, with $d_{\mathrm{e}} = d \times \tilde{d}$, it can be reformulated by decomposing the summation over k into two separate summations over indices i and j, with the definition of $k = i\tilde{d} + j$, as follows

$$\left|\psi_{\mathrm{E}}\right\rangle = \hat{\mathrm{E}}\left|\psi\right\rangle = \sum_{i=0}^{d-1} \sum_{j=0}^{\tilde{d}-1} \xi_{i,j} \left|i\tilde{d} + j\right\rangle_L \,, \tag{B.2}$$

where $\xi_{i,j} = \xi'_k$. The next step involves establishing a connection between the coefficients of the expanded quantum state $\left|\psi_{\mathrm{E}}\right\rangle$, denoted as $\xi_{i,j}$, and the coefficients of the original quantum state $\left|\psi\right\rangle$, represented as ξ_i. To achieve this, the $d_{\mathrm{e}} \times d$, i.e., $(d \times \tilde{d}) \times (d \times 1)$ mode expansion Kraus operator is considered, which is defined by Eq.(18) as follows

$$\hat{\mathrm{E}} = \hat{\mathbb{1}} \otimes |u_0\rangle \,, \tag{B.3}$$

where $\hat{\mathbb{1}}$ denotes the $d \times d$ identity operator, and $|u_0\rangle$ is a $\tilde{d} \times 1$ column vector $\begin{bmatrix} 1 & 0 & 0 & \dots & 0 \end{bmatrix}^\top$. Consequently, the matrix elements $e_{k,i}$ derived from Eq.(B.3), located in the k-th row and i-th column, for $0 \leq k < d_{\mathrm{e}}$ and $0 \leq i < d$, are characterized as follows

$$e_{k,i} = \delta_{k,i\tilde{d}} = \begin{cases} 1 & k = i\tilde{d}, \\ 0 & \text{otherwise.} \end{cases} \tag{B.4}$$

Therefore, using Eq.(B.1) and the definition of $k = i\tilde{d} + j$, one can deduce

$$\xi_{i,j} = \xi'_k = \sum_{i=0}^{d-1} e_{k,i} \, \xi_i = \xi_i \, \delta_{j,0}. \tag{B.5}$$

B.1. Deriving the Coefficients of the Quantum Signal State

In the following, we derive the relationship between the quantum signal $\left|\psi^{(\mathrm{m})}\right\rangle$ and the expanded state $\left|\psi_{\mathrm{E}}^{(\mathrm{m},\tilde{\mathrm{m}})}\right\rangle$. First, consider applying the mode expansion operator $\hat{\mathrm{E}}^{(\mathrm{m})\to(\mathrm{m},\tilde{\mathrm{m}})}$, as defined in Eq.(12), to two arbitrary quantum states $\left|\psi^{(\mathrm{m})}\right\rangle$ and $\left|\phi^{(\mathrm{m})}\right\rangle$, i.e.,

$$\hat{\mathrm{E}}^{(\mathrm{m})\to(\mathrm{m},\tilde{\mathrm{m}})} \left|\psi^{(\mathrm{m})}\right\rangle = \left|\psi^{(\mathrm{m})}\right\rangle_{\tilde{m}_0} |0\rangle_{\tilde{m}_1} |0\rangle_{\tilde{m}_2} \dots |0\rangle_{\tilde{m}_{\tilde{d}-1}} \tag{B.6}$$

and

$$\hat{\mathrm{E}}^{(\mathrm{m})\to(\mathrm{m},\tilde{\mathrm{m}})} \left|\phi^{(\mathrm{m})}\right\rangle = \left|\phi^{(\mathrm{m})}\right\rangle_{\tilde{m}_0} |0\rangle_{\tilde{m}_1} |0\rangle_{\tilde{m}_2} \dots |0\rangle_{\tilde{m}_{\tilde{d}-1}} \,. \tag{B.7}$$

Taking the conjugate transpose of Eq.(B.7) and multiplying it by Eq.(B.6) yields

$$\left\langle \phi^{(\mathrm{m})} \right| \hat{\mathrm{E}}^{\dagger(\mathrm{m})\to(\mathrm{m},\tilde{\mathrm{m}})} \hat{\mathrm{E}}^{(\mathrm{m})\to(\mathrm{m},\tilde{\mathrm{m}})} \left| \psi^{(\mathrm{m})} \right\rangle = {}_{\tilde{m}_0}\left\langle \phi^{(\mathrm{m})} \right| \left. \psi^{(\mathrm{m})} \right\rangle_{\tilde{m}_0} . \tag{B.8}$$

Since Eq.(B.8) holds for arbitrary quantum states $\left|\psi^{(\mathrm{m})}\right\rangle$ and $\left|\phi^{(\mathrm{m})}\right\rangle$, it is concluded that

$$\hat{\mathrm{E}}^{\dagger(\mathrm{m})\to(\mathrm{m},\tilde{\mathrm{m}})} \hat{\mathrm{E}}^{(\mathrm{m})\to(\mathrm{m},\tilde{\mathrm{m}})} = \hat{\mathbb{1}}^{(\mathrm{m})}. \tag{B.9}$$

The expanded signal state can be represented as follows

$$\begin{aligned} \left|\psi_{\mathrm{E}}^{(\mathrm{m},\tilde{\mathrm{m}})}\right\rangle &= \hat{\mathrm{E}}^{(\mathrm{m})\to(\mathrm{m},\tilde{\mathrm{m}})} \left|\psi^{(\mathrm{m})}\right\rangle = \hat{\mathrm{E}}^{(\mathrm{m})\to(\mathrm{m},\tilde{\mathrm{m}})} f\left(\hat{a}_{\xi}^{\dagger(\mathrm{m})}\right) \hat{\mathrm{E}}^{\dagger(\mathrm{m})\to(\mathrm{m},\tilde{\mathrm{m}})} |0\rangle \\ &= f\left(\sum_{i=0}^{d-1} \xi_i \hat{\mathrm{E}}^{(\mathrm{m})\to(\mathrm{m},\tilde{\mathrm{m}})} \hat{a}_{m_i}^{\dagger} \hat{\mathrm{E}}^{\dagger(\mathrm{m})\to(\mathrm{m},\tilde{\mathrm{m}})}\right)|0\rangle , \end{aligned} \tag{B.10}$$

where $\hat{\mathrm{E}}^{\dagger(\mathrm{m})\to(\mathrm{m},\tilde{\mathrm{m}})} |0\rangle = |0\rangle$, Eq.(3), and Eq.(A.4) are used. Notice in the derivation of Eq.(A.4), as well as Eq.(A.7), only the $\hat{\mathrm{U}}^{\dagger}\hat{\mathrm{U}} = \hat{\mathbb{1}}$ relation is employed, which is a property satisfied by the Kraus operator $\hat{\mathrm{E}}^{(\mathrm{m})\to(\mathrm{m},\tilde{\mathrm{m}})}$, as indicated in Eq.(B.9). Furthermore, by employing the field transformation matrix similar to Eq.(A.7), Eq.(B.10) can be simplified to

$$\left|\psi_{\mathrm{E}}^{(\mathrm{m},\tilde{\mathrm{m}})}\right\rangle = f\left(\sum_{i=0}^{d-1}\sum_{k=0}^{d_{\mathrm{e}}-1} \xi_i \; e_{k,i} \; \hat{a}_{m_k}^{\dagger}\right)|0\rangle = f\left(\sum_{k=0}^{d_{\mathrm{e}}-1} \bar{\xi}_k \hat{a}_{m_k}^{\dagger}\right)|0\rangle , \tag{B.11}$$

where using Eq.(B.4), we have

$$\bar{\xi}_k = \sum_{i=0}^{d-1} \xi_i e_{k,i} = \begin{cases} \xi_i & k = i\tilde{d}, \\ 0 & \text{otherwise.} \end{cases} \tag{B.12}$$

Equation (B.11) can be reformulated into the standard form presented in Eq.(12) as follows

$$\left|\psi_{\mathrm{E}}^{(\mathrm{m},\tilde{\mathrm{m}})}\right\rangle = f\left(\sum_{i=0}^{d-1}\sum_{j=0}^{\tilde{d}-1} \xi_{i,j} \; \hat{a}_{m_i,\tilde{m}_j}^{\dagger}\right)|0\rangle . \tag{B.13}$$

This transformation involves separating the summation over k into two distinct summations over i and j, where $k = i\tilde{d} + j$. We define $\hat{a}_{m_k}^{\dagger} = \hat{a}_{m_i,\tilde{m}_j}^{\dagger}$ and $\bar{\xi}_k = \xi_{i,j}$. According to Eq.(B.12), this leads to

$$\xi_{i,j} = \xi_i \; \delta_{j,0} = \begin{cases} \xi_i & j = 0, \\ 0 & \text{otherwise.} \end{cases} \tag{B.14}$$

This corresponds to Eq.(16) and confirms the result of the informational coefficients in Eq.(B.5).

C. The Mode Reduction Procedure

In this section, the quantum source is represented by either a single photon or a coherent state, as employed in most quantum communication applications, such as quantum key distribution or quantum secure direct communication. In the two following subsections, the mode reduction procedure for these quantum states are explored.

C.1. Quantum Coherent State

For the coherent state with the creation operator $\hat{a}_{\xi}^{\dagger(\mathrm{m},\tilde{\mathrm{m}})}$, the Fock state distribution function, analogous to Eq.(4), is given by

$$f_{\alpha}\left(\hat{a}_{\xi}^{\dagger(\mathrm{m},\tilde{\mathrm{m}})}\right) = e^{-\frac{|\alpha|^2}{2}} e^{\alpha\, \hat{a}_{\xi}^{\dagger(\mathrm{m},\tilde{\mathrm{m}})}}, \tag{C.1}$$

where using Eq.(12), the creation operator $\hat{a}_{\xi}^{\dagger(\mathrm{m},\tilde{\mathrm{m}})}$ in the expanded space $(\mathrm{m},\tilde{\mathrm{m}})$ is defined as

$$\hat{a}_{\xi}^{\dagger(\mathrm{m},\tilde{\mathrm{m}})} = \sum_{i=0}^{d-1}\sum_{j=0}^{\tilde{d}-1} \xi_{i,j}\; \hat{a}^{\dagger}_{m_i,\tilde{m}_j}. \tag{C.2}$$

The probability of obtaining n photons when measuring a coherent state characterized by the complex parameter α follows a Poisson distribution with an average of $|\alpha|^2$ [49]. Substituting Eq.(C.2) into Eq.(C.1), the quantum coherent state can be articulated as follows

$$\begin{aligned}\left|\psi^{(\mathrm{m},\tilde{\mathrm{m}})}\right\rangle &= f_{\alpha}\left(\hat{a}_{\xi}^{\dagger(\mathrm{m},\tilde{\mathrm{m}})}\right)|0\rangle = e^{-\frac{|\alpha|^2}{2}} e^{\alpha \sum_{i=0}^{d-1}\sum_{j=0}^{\tilde{d}-1} \xi_{i,j}\; \hat{a}^{\dagger}_{m_i,\tilde{m}_j}}|0\rangle = \prod_{i=0}^{d-1}\prod_{j=0}^{\tilde{d}-1} e^{-\frac{|\alpha|^2}{2}} e^{\alpha\xi_{i,j}\; \hat{a}^{\dagger}_{m_i,\tilde{m}_j}}|0\rangle \\ &= \prod_{i=0}^{d-1}\prod_{j=0}^{\tilde{d}-1} \left|\alpha\; \xi_{i,j}\right\rangle_{m_i,\tilde{m}_j},\end{aligned} \tag{C.3}$$

where the normalization condition of Eq.(14) is used.

To achieve the reduced Hilbert space associated with the quantum state, thereby eliminating the components corresponding to the mode $\tilde{m}_J$, for $0 \le J < \tilde{d}$ and $J \neq j_0$, it is essential to perform a partial trace of the state. This process involves considering the relevant density operator of the quantum state, specifically expressed as follows

$$\rho^{(\mathrm{m},\tilde{\mathrm{m}})} = \left|\psi^{(\mathrm{m},\tilde{\mathrm{m}})}\right\rangle\!\!\left\langle\psi^{(\mathrm{m},\tilde{\mathrm{m}})}\right| = \prod_{i=0}^{d-1}\prod_{j=0}^{\tilde{d}-1} \left|\alpha\; \xi_{i,j}\right\rangle_{m_i,\tilde{m}_j}\!\left\langle\alpha\; \xi_{i,j}\right|. \tag{C.4}$$

Therefore, the reduced density operator is given by

$$\begin{aligned}\rho^{(\mathrm{m})}_{\tilde{m}_{j_0}} &= \hat{\mathrm{R}}^{(\mathrm{m},\tilde{\mathrm{m}})\to(\mathrm{m})}_{\tilde{m}_{j_0}}\, \rho^{(\mathrm{m},\tilde{\mathrm{m}})}\, \hat{\mathrm{R}}^{\dagger(\mathrm{m},\tilde{\mathrm{m}})\to(\mathrm{m})}_{\tilde{m}_{j_0}} = \mathrm{Tr}_{(m_I,\tilde{m}_J)\in\mathcal{T}}\left\{\prod_{i=0}^{d-1}\prod_{j=0}^{\tilde{d}-1} \left|\alpha\; \xi_{i,j}\right\rangle_{m_i,\tilde{m}_j}\!\left\langle\alpha\; \xi_{i,j}\right|\right\} \\ &= \prod_{i=0}^{d-1} \left|\alpha\; \xi_{i,j_0}\right\rangle_{m_i,\tilde{m}_{j_0}}\!\left\langle\alpha\; \xi_{i,j_0}\right|,\end{aligned} \tag{C.5}$$

where the set $\mathcal{T}$ is defined in Eq.(30). Since the coherent state is factorizable, it does not display any entanglement characteristics. Equation (C.5) results in a pure state

$$\left|\psi^{(\mathrm{m})}\right\rangle_{\tilde{m}_{j_0}} = \hat{\mathrm{R}}^{(\mathrm{m},\tilde{\mathrm{m}})\to(\mathrm{m})}_{\tilde{m}_{j_0}} \left|\psi^{(\mathrm{m},\tilde{\mathrm{m}})}\right\rangle = \prod_{i=0}^{d-1} \left|\alpha\; \xi_{i,j_0}\right\rangle_{m_i,\tilde{m}_{j_0}}. \tag{C.6}$$

Eliminating the common mode $\tilde{m}_{j_0}$ from Eq.(C.6) yields

$$\begin{aligned}\left|\psi^{(\mathrm{m})}\right\rangle &= \hat{\mathrm{R}}^{(\mathrm{m},\tilde{\mathrm{m}})\to(\mathrm{m})}_{\tilde{m}_{j_0}} \left|\psi^{(\mathrm{m},\tilde{\mathrm{m}})}\right\rangle = \prod_{i=0}^{d-1} \left|\alpha\; \xi_{i,j_0}\right\rangle_{m_i} = \prod_{i=0}^{d-1} e^{-\frac{|\alpha\; \xi_{i,j_0}|^2}{2}} e^{\alpha\xi_{i,j_0}\; \hat{a}^{\dagger}_{m_i}}|0\rangle \\ &= e^{-\sum_{i=0}^{d-1}\frac{|\alpha\; \xi_{i,j_0}|^2}{2}} e^{\alpha \sum_{i=0}^{d-1} \xi_{i,j_0}\; \hat{a}^{\dagger}_{m_i}}|0\rangle = f_{\alpha\xi_{j_0}}\left(\hat{a}^{\dagger(\mathrm{m})}_{\xi'}\right)|0\rangle,\end{aligned} \tag{C.7}$$

where

$$\hat{a}^{\dagger(\mathrm{m})}_{\xi'} = \sum_{i=0}^{d-1} \frac{\xi_{i,j_0}}{\tilde{\xi}_{j_0}}\, \hat{a}^{\dagger}_{m_i} \tag{C.8}$$

and

$$\tilde{\xi}_{j_0} = \left(\sum_{i=0}^{d-1} |\xi_{i,j_0}|^2 \right)^{1/2}. \tag{C.9}$$

Consequently, the average value of the Poisson distribution, which represents the probability of detecting n photons, diminishes from $|\alpha|^2$ to $|\alpha\tilde{\xi}_{j_0}|^2$.

C.2. Single Photon State

In contrast, for a single photon represented by the creation operator $\hat{a}^{\dagger(\mathrm{m},\tilde{\mathrm{m}})}_{\xi}$, the function that describes this state is defined as the identity function, analogous to Eq.(5), as follows

$$f(\hat{a}^{\dagger(\mathrm{m},\tilde{\mathrm{m}})}_{\xi}) = \hat{a}^{\dagger(\mathrm{m},\tilde{\mathrm{m}})}_{\xi}. \tag{C.10}$$

Consequently, the single photon state can be represented as

$$\left|\psi^{(\mathrm{m},\tilde{\mathrm{m}})}\right\rangle = \sum_{i=0}^{d-1} \sum_{j=0}^{\tilde{d}-1} \xi_{i,j}\, \hat{a}^{\dagger}_{m_i,\tilde{m}_j} |0\rangle . \tag{C.11}$$

This leads to the following form of the density operator

$$\rho^{(\mathrm{m},\tilde{\mathrm{m}})} = \sum_{i,i'} \sum_{j,j'} \xi_{i,j}\, \xi^{*}_{i',j'}\, \hat{a}^{\dagger}_{m_i,\tilde{m}_j} |0\rangle\langle 0|\, \hat{a}_{m_{i'},\tilde{m}_{j'}}. \tag{C.12}$$

Therefore, the reduced density operator is given by

$$\rho^{(\mathrm{m})}_{\tilde{m}_{j_0}} = \hat{\mathrm{R}}^{(\mathrm{m},\tilde{\mathrm{m}})\to(\mathrm{m})}_{\tilde{m}_{j_0}} \rho^{(\mathrm{m},\tilde{\mathrm{m}})}\, \hat{\mathrm{R}}^{\dagger(\mathrm{m},\tilde{\mathrm{m}})\to(\mathrm{m})}_{\tilde{m}_{j_0}} = \mathrm{Tr}_{(m_I,\tilde{m}_J)\in\mathcal{T}} \left\{ \rho^{(\mathrm{m},\tilde{\mathrm{m}})} \right\}. \tag{C.13}$$

Tracing over all modes $(m_I, \tilde{m}_J) \in \mathcal{T}$ for a single-photon density operator is equivalent to aggregating the expectation values associated with the various number states within $\mathcal{T}$. This basis comprises single-photon states linked to modes $(m_I, \tilde{m}_J) \in \mathcal{T}$, specifically, $d(\tilde{d}-1)$ single-photon states, which can be expressed as

$$|1\rangle_{m_I,\tilde{m}_J} = \hat{a}^{\dagger}_{m_I,\tilde{m}_J} \left|0_{\bar{j}_0}\right\rangle, \tag{C.14}$$

where $\left|0_{\bar{j}_0}\right\rangle$ represents the tensor product of $d(\tilde{d}-1)$ vacuum states corresponding to modes $(m_I, \tilde{m}_J) \in \mathcal{T}$, i.e.,

$$\left|0_{\bar{j}_0}\right\rangle = \prod_{I=0}^{d-1} \prod_{\substack{J=0 \\ J\neq j_0}}^{\tilde{d}-1} |0\rangle_{m_I,\tilde{m}_J}. \tag{C.15}$$

Furthermore, since the single photon can exist in modes beyond those in $\mathcal{T}$, the basis for which expectation values must be calculated also includes the vacuum state itself. Consequently, Eq.(C.13) becomes

$$\rho^{(\mathrm{m})}_{\tilde{m}_{j_0}} = \sum_{I=0}^{d-1} \sum_{\substack{J=0 \\ J\neq j_0}}^{\tilde{d}-1} \left\langle 0_{\bar{j}_0} \right| \hat{a}_{m_I,\tilde{m}_J}\, \rho^{(\mathrm{m},\tilde{\mathrm{m}})}\, \hat{a}^{\dagger}_{m_I,\tilde{m}_J} \left|0_{\bar{j}_0}\right\rangle + \left\langle 0_{\bar{j}_0} \right| \rho^{(\mathrm{m},\tilde{\mathrm{m}})} \left|0_{\bar{j}_0}\right\rangle. \tag{C.16}$$

The first term in Eq.(C.16) is computed as follows

$$\sum_{I=0}^{d-1}\sum_{\substack{J=0\\J\neq j_0}}^{\tilde{d}-1}\left\langle 0_{\bar{j}_0}\right|\hat{a}_{m_I,\tilde{m}_J}\,\rho^{(\mathrm{m},\tilde{\mathrm{m}})}\,\hat{a}^{\dagger}_{m_I,\tilde{m}_J}\left|0_{\bar{j}_0}\right\rangle = \sum_{i,i',I}\sum_{\substack{j,j',J\\J\neq j_0}}\xi_{i,j}\xi^{*}_{i',j'}\left\langle 0_{\bar{j}_0}\right|\hat{a}_{m_I,\tilde{m}_J}\hat{a}^{\dagger}_{m_i,\tilde{m}_j}|0\rangle\langle 0|\,\hat{a}_{m_{i'},\tilde{m}_{j'}}$$
$$\times\,\hat{a}^{\dagger}_{m_I,\tilde{m}_J}\left|0_{\bar{j}_0}\right\rangle$$
$$=\sum_{i,i',I}\sum_{\substack{j,j',J\\J\neq j_0}}\xi_{i,j}\xi^{*}_{i',j'}\left(\delta_{i,I}\delta_{j,J}\,|0\rangle_{m_i,\tilde{m}_{j_0}}\right)\left(\delta_{i',I}\delta_{j',J}\,\langle 0|_{m_{i'},\tilde{m}_{j_0}}\right)=\sum_{i=0}^{d-1}\sum_{\substack{j=0\\j\neq j_0}}^{\tilde{d}-1}|\xi_{i,j}|^2\left|0_{j_0}\right\rangle\!\left\langle 0_{j_0}\right|, \quad \text{(C.17)}$$

where $\left|0_{j_0}\right\rangle$ denotes the tensor product of d vacuum states associated with modes $(m_i, \tilde{m}_{j_0})$, i.e.,

$$\left|0_{j_0}\right\rangle=\prod_{i=0}^{d-1}|0\rangle_{m_i,\tilde{m}_{j_0}}\,. \quad \text{(C.18)}$$

Additionally, the second term of Eq.(C.16) is expressed as follows

$$\left\langle 0_{\bar{j}_0}\right|\rho^{(\mathrm{m},\tilde{\mathrm{m}})}\left|0_{\bar{j}_0}\right\rangle=\sum_{i,i'}\sum_{j,j'}\xi_{i,j}\xi^{*}_{i',j'}\left\langle 0_{\bar{j}_0}\right|\hat{a}^{\dagger}_{m_i,\tilde{m}_j}|0\rangle\langle 0|\,\hat{a}_{m_{i'},\tilde{m}_{j'}}\left|0_{\bar{j}_0}\right\rangle$$
$$=\sum_{i,i'}\xi_{i,j_0}\xi^{*}_{i',j_0}\hat{a}^{\dagger}_{m_i,\tilde{m}_{j_0}}\left|0_{j_0}\right\rangle\!\left\langle 0_{j_0}\right|\hat{a}_{m_{i'},\tilde{m}_{j_0}}. \quad \text{(C.19)}$$

Thus, the reduced density operator by substituting Eq.(C.17) and Eq.(C.19) into Eq.(C.16), and rewriting $\left|0_{j_0}\right\rangle$ simply as $|0\rangle$, is given by

$$\rho^{(\mathrm{m})}_{\tilde{m}_{j_0}}=\sum_{i,i'}\xi_{i,j_0}\xi^{*}_{i',j_0}\hat{a}^{\dagger}_{m_i,\tilde{m}_{j_0}}\,|0\rangle\langle 0|\,\hat{a}_{m_{i'},\tilde{m}_{j_0}}+\sum_{i=0}^{d-1}\sum_{\substack{j=0\\j\neq j_0}}^{\tilde{d}-1}|\xi_{i,j}|^2\,|0\rangle\langle 0|\,. \quad \text{(C.20)}$$

The first term in Eq.(C.20) implies that with a probability p, which will be specified in the following, the single photon is found in the desired mode j_0. In contrast, the second term indicates that with a probability of $1-p$, the photon resides in any of the other blocked modes, excluding the desired mode j_0. The probability of finding a single photon in mode $\tilde{m}_{j_0}$ is determined by the sum of the elements along the main diagonal corresponding to the first term of Eq.(C.20). This is expressed as

$$p=\sum_{i=0}^{d-1}|\xi_{i,j_0}|^2=|\tilde{\xi}_{j_0}|^2, \quad \text{(C.21)}$$

where Eq.(C.9) is used. This signifies that the success probability for the mode reduction of the single photon, defined as the probability of finding the state in the desired mode j_0, is given by

$$\mathcal{S}=p=|\tilde{\xi}_{j_0}|^2. \quad \text{(C.22)}$$

Moreover, conditioned on the successful execution of the mode reduction operation, the reduced density operator can be formulated in accordance with the fifth postulate of quantum mechanics [48] as

$$\rho'^{(\mathrm{m})}_{\tilde{m}_{j_0}}=\sum_{i,i'}\frac{\xi_{i,j_0}\xi^{*}_{i',j_0}}{|\tilde{\xi}_{j_0}|^2}\hat{a}^{\dagger}_{m_i,\tilde{m}_{j_0}}\,|0\rangle\langle 0|\,\hat{a}_{m_{i'},\tilde{m}_{j_0}}\,. \quad \text{(C.23)}$$

Equation (C.23) represents a pure quantum state given by

$$\left|\psi^{(\mathrm{m})}\right\rangle_{\tilde{m}_{j_0}} = \hat{\mathrm{R}}^{(\mathrm{m},\tilde{\mathrm{m}})\to(\mathrm{m})}_{\tilde{m}_{j_0}} \left|\psi^{(\mathrm{m},\tilde{\mathrm{m}})}\right\rangle = \sum_{i=0}^{d-1} \frac{\xi_{i,j_0}}{\tilde{\xi}_{j_0}} \hat{a}^{\dagger}_{m_i,\tilde{m}_{j_0}} |0\rangle \,, \tag{C.24}$$

which is identical to the desired reduced state $\left|\psi^{(\mathrm{m})}_{\mathrm{D}}\right\rangle_{\tilde{m}_{j_0}}$ in Eq.(31). Dropping the common mode $\tilde{m}_{j_0}$ from Eq.(C.24) gives

$$\left|\psi^{(\mathrm{m})}\right\rangle = \hat{\mathrm{R}}^{(\mathrm{m},\tilde{\mathrm{m}})\to(\mathrm{m})}_{\tilde{m}_{j_0}} \left|\psi^{(\mathrm{m},\tilde{\mathrm{m}})}\right\rangle = \sum_{i=0}^{d-1} \frac{\xi_{i,j_0}}{\tilde{\xi}_{j_0}} \hat{a}^{\dagger}_{m_i} |0\rangle = f\left(\sum_{i=0}^{d-1} \frac{\xi_{i,j_0}}{\tilde{\xi}_{j_0}} \hat{a}^{\dagger}_{m_i}\right)|0\rangle = f\left(\hat{a}^{\dagger(\mathrm{m})}_{\xi}\right)|0\rangle \,, \tag{C.25}$$

with $\mathcal{S} = |\tilde{\xi}_{j_0}|^2$.

References

1. C. H. Bennett and G. Brassard, "Quantum cryptography: public key distribution and coin tossing," in *Conf. on Computers, Systems and Signal Processing ,(Bangalore) India,* vol. 175 (1984).
2. A. K. Ekert, "Quantum cryptography based on bell's theorem," Phys. review letters **67**, 661 (1991).
3. S. Haroche and J.-M. Raimond, *Exploring the quantum: atoms, cavities, and photons* (Oxford university press, 2006).
4. M. Kjaergaard, M. E. Schwartz, J. Braumüller, *et al.*, "Superconducting qubits: Current state of play," Annu. Rev. Condens. Matter Phys. **11**, 369–395 (2020).
5. J. L. O'brien, "Optical quantum computing," Science **318**, 1567–1570 (2007).
6. B. Da Lio, D. Cozzolino, N. Biagi, *et al.*, "Path-encoded high-dimensional quantum communication over a 2-km multicore fiber," npj Quantum Inf. **7**, 63 (2021).
7. A. Duplinskiy, V. Ustimchik, A. Kanapin, *et al.*, "Low loss qkd optical scheme for fast polarization encoding," Opt. express **25**, 28886–28897 (2017).
8. F. Grünenfelder, A. Boaron, D. Rusca, *et al.*, "Simple and high-speed polarization-based qkd," Appl. Phys. Lett. **112** (2018).
9. C. Agnesi, M. Avesani, L. Calderaro, *et al.*, "Simple quantum key distribution with qubit-based synchronization and a self-compensating polarization encoder," Optica **7**, 284–290 (2020).
10. T. Zhang, Z.-Q. Yin, Z.-F. Han, and G.-C. Guo, "A frequency-coded quantum key distribution scheme," Opt. communications **281**, 4800–4802 (2008).
11. H.-H. Lu, M. Liscidini, A. L. Gaeta, *et al.*, "Frequency-bin photonic quantum information," Optica **10**, 1655–1671 (2023).
12. M. Lucamarini, K. Patel, J. Dynes, *et al.*, "Efficient decoy-state quantum key distribution with quantified security," Opt. express **21**, 24550–24565 (2013).
13. N. T. Islam, C. C. W. Lim, C. Cahall, *et al.*, "Provably secure and high-rate quantum key distribution with time-bin qudits," Sci. advances **3**, e1701491 (2017).
14. F. Bouchard, D. England, P. J. Bustard, *et al.*, "Quantum communication with ultrafast time-bin qubits," PRX Quantum **3**, 010332 (2022).
15. M. Reck, A. Zeilinger, H. J. Bernstein, and P. Bertani, "Experimental realization of any discrete unitary operator," Phys. review letters **73**, 58 (1994).
16. M. Rezai and J. A. Salehi, "Quantum computation via multiport discretized quantum fourier optical processors," IEEE Trans. on Quantum Eng. (2023).
17. J. M. Lukens and P. Lougovski, "Frequency-encoded photonic qubits for scalable quantum information processing," Optica **4**, 8–16 (2017).
18. H.-H. Lu, J. M. Lukens, N. A. Peters, *et al.*, "Electro-optic frequency beam splitters and tritters for high-fidelity photonic quantum information processing," Phys. review letters **120**, 030502 (2018).
19. A. Crespi, R. Ramponi, R. Osellame, *et al.*, "Integrated photonic quantum gates for polarization qubits," Nat. communications **2**, 566 (2011).
20. J. Wang, D. Bonneau, M. Villa, *et al.*, "Chip-to-chip quantum photonic interconnect by path-polarization interconversion," Optica **3**, 407–413 (2016).
21. D. Deutsch, "Quantum theory, the church–turing principle and the universal quantum computer," Proc. Royal Soc. London. A. Math. Phys. Sci. **400**, 97–117 (1985).
22. M. A. Nielsen and I. L. Chuang, *Quantum computation and quantum information*, vol. 2 (Cambridge university press Cambridge, 2001).
23. M. Nakahara and T. Ohmi, *Quantum computing: from linear algebra to physical realizations* (CRC press, 2008).
24. N. Gisin, G. Ribordy, W. Tittel, and H. Zbinden, "Quantum cryptography," Rev. modern physics **74**, 145 (2002).

25. M. Razavi, *An Introduction to Quantum Communications Networks: Or, how shall we communicate in the quantum era?* (Morgan & Claypool Publishers, 2018).
26. F. Xu, X. Ma, Q. Zhang, *et al.*, "Secure quantum key distribution with realistic devices," Rev. modern physics **92**, 025002 (2020).
27. R. Wolf, "Quantum key distribution," Lect. notes physics **988** (2021).
28. Y. Cao, Y. Zhao, Q. Wang, *et al.*, "The evolution of quantum key distribution networks: On the road to the qinternet," IEEE Commun. Surv. & Tutorials **24**, 839–894 (2022).
29. I. B. Djordjevic, *Quantum Communication, Quantum Networks, and Quantum Sensing* (Academic Press, 2022).
30. C. H. Bennett and S. J. Wiesner, "Communication via one-and two-particle operators on einstein-podolsky-rosen states," Phys. review letters **69**, 2881 (1992).
31. C. H. Bennett, G. Brassard, C. Crépeau, *et al.*, "Teleporting an unknown quantum state via dual classical and einstein-podolsky-rosen channels," Phys. review letters **70**, 1895 (1993).
32. M. Hillery, V. Bužek, and A. Berthiaume, "Quantum secret sharing," Phys. Rev. A **59**, 1829 (1999).
33. L. Xiao, G. Lu Long, F.-G. Deng, and J.-W. Pan, "Efficient multiparty quantum-secret-sharing schemes," Phys. Rev. A-Atomic, Mol. Opt. Phys. **69**, 052307 (2004).
34. G.-L. Long and X.-S. Liu, "Theoretically efficient high-capacity quantum-key-distribution scheme," Phys. Rev. A **65**, 032302 (2002).
35. F.-G. Deng, G. L. Long, and X.-S. Liu, "Two-step quantum direct communication protocol using the einstein-podolsky-rosen pair block," Phys. Rev. A **68**, 042317 (2003).
36. D. Pan, G.-L. Long, L. Yin, *et al.*, "The evolution of quantum secure direct communication: on the road to the qinternet," IEEE Commun. Surv. & Tutorials (2024).
37. H. J. Kimble, "The quantum internet," Nature **453**, 1023–1030 (2008).
38. F. Grosshans and P. Grangier, "Continuous variable quantum cryptography using coherent states," Phys. review letters **88**, 057902 (2002).
39. F. Grosshans, G. Van Assche, J. Wenger, *et al.*, "Quantum key distribution using gaussian-modulated coherent states," Nature **421**, 238–241 (2003).
40. Y. Zhang, Z. Chen, S. Pirandola, *et al.*, "Long-distance continuous-variable quantum key distribution over 202.81 km of fiber," Phys. review letters **125**, 010502 (2020).
41. A. Boaron, B. Korzh, R. Houlmann, *et al.*, "Simple 2.5 ghz time-bin quantum key distribution," Appl. Phys. Lett. **112**, 171108 (2018).
42. N. K. Pathak, S. Chaudhary, Sangeeta, and B. Kanseri, "Phase encoded quantum key distribution up to 380 km in standard telecom grade fiber enabled by baseline error optimization," Sci. Reports **13**, 15868 (2023).
43. M. Mafu, A. Dudley, S. Goyal, *et al.*, "Higher-dimensional orbital-angular-momentum-based quantum key distribution with mutually unbiased bases," Phys. Rev. A **88**, 032305 (2013).
44. F. Bouchard, N. H. Valencia, F. Brandt, *et al.*, "Measuring azimuthal and radial modes of photons," Opt. express **26**, 31925–31941 (2018).
45. J. Cariñe, G. Cañas, P. Skrzypczyk, *et al.*, "Multi-core fiber integrated multi-port beam splitters for quantum information processing," Optica **7**, 542–550 (2020).
46. R. J. Glauber, "Coherent and incoherent states of the radiation field," Phys. Rev. **131**, 2766 (1963).
47. M. Rezai and J. A. Salehi, "Quantum CDMA communication systems," IEEE Trans. on Inf. Theory **67**, 5526–5547 (2021).
48. C. Cohen-Tannoudji, B. Diu, and F. Laloe, "Quantum mechanics, volume 1: Basic concepts, tools, and applications," Quantum Mech. **1**, 898 (1986).
49. G. Cariolaro, *Quantum communications* (Springer, 2015).
50. A. Ekert, T. Hosgood, A. Kay, and C. Macchiavello, "Introduction to quantum information science," https://qubit.guide.
51. M. M. Wilde, *Quantum information theory* (Cambridge university press, 2013).
52. A. Tomita, K.-i. Yoshino, Y. Nambu, *et al.*, "High speed quantum key distribution system," Opt. Fiber Technol. **16**, 55–62 (2010).
53. F. Bouchard, K. Bonsma-Fisher, K. Heshami, *et al.*, "Measuring ultrafast time-bin qudits," Phys. Rev. A **107**, 022618 (2023).
54. D. England, F. Bouchard, K. Fenwick, *et al.*, "Perspectives on all-optical kerr switching for quantum optical applications," Appl. Phys. Lett. **119**, 160501 (2021).
55. X. Tang, "Optically switched quantum key distribution network," Ph.D. thesis (2019).
56. A. Dixon, Z. Yuan, J. Dynes, *et al.*, "Gigahertz decoy quantum key distribution with 1 mbit/s secure key rate," Opt. express **16**, 18790–18797 (2008).
57. Z. Yuan, A. Dixon, J. Dynes, *et al.*, "Practical gigahertz quantum key distribution based on avalanche photodiodes," New J. Phys. **11**, 045019 (2009).
58. J. Dynes, A. Wonfor, W.-S. Tam, *et al.*, "Cambridge quantum network," npj Quantum Inf. **5**, 101 (2019).
59. U. Leonhardt, *Measuring the quantum state of light*, vol. 22 (Cambridge university press, 1997).
60. R. Loudon, *The quantum theory of light* (OUP Oxford, 2000).
61. A. Furusawa and A. Furusawa, *Quantum states of light* (Springer, 2015).